Lawrence Berkeley National Laboratory
Recent Work

Title
Experimental Study of Toxic Waste Incineration

Permalink
https://escholarship.org/uc/item/8sf6k29m

Author
Taga, K.

Publication Date
1989-08-01

Lawrence Berkeley Laboratory
UNIVERSITY OF CALIFORNIA

APPLIED SCIENCE DIVISION
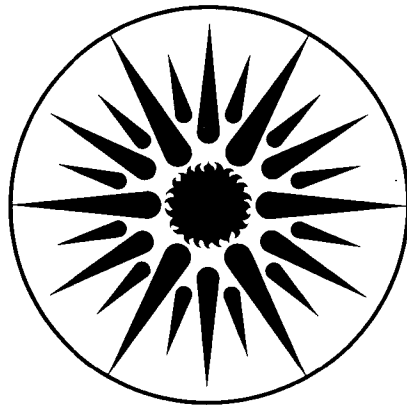
Experimental Study of Toxic Waste Incineration

K. Taga

(M.S. Thesis)

August 1989

APPLIED SCIENCE DIVISION

DISCLAIMER

EXPERIMENTAL STUDY OF TOXIC

WASTE INCINERATION

by

Karim Taga

LAWRENCE BERKELEY LABORATORY
Applied Science Division

ECOLE SUPERIEURE DE L'ENERGIE ET DES MATERIAUX
Option Energetique Industrielle

March - August 1989

ABSTRACT

We have recently begun a study of the thermal destruction
of toxic wastes. One of the goals of the project is to
develop methods for the measurement of species important
in the combustion of chlorinated hydrocarbons. We are
investigating the use of infrared absorption spectroscopy
for this purpose, with emphasis on Fourier-transform
infrared spectroscopy (FTIR) coupled with long path length
cells. This combination should permit the simultaneous
quantitative determination of a large number of compounds,
in particular simple C_1 and C_2 chlorinated hydrocarbons.

We have obtained infrared spectra for a number of
chlorinated species, and for the expected products of their
pyrolysis and oxidation. Spectra are recorded on a Digilab
FTS-40 spectrometer with a cooled MCT detector and 0.25 cm^{-1}
resolution. Samples are held in a conventional 10 cm gas
cell or an adjustable path length (maximum 22.8 m) cell from
Infrared Analysis, Inc., fitted with ZnSe windows. We have
determined effects of resolution, pressure, temperature, and
gas composition on the resulting spectra, and have

1

determined sensitivity limits, pressure broadening, and instrument linearity for several species. For example, we have measured ethyl chloride at the 400 ppb level, and have determined that the measurement of this species is linear up to the percent range.

Spectra of products from our combustion driven flow reactor have also been measured. Samples are withdrawn through stainless steel probes and transferred to the long path cell maintained at 100 torr to prevent water condensation.

Ethyl chloride (C_2H_5Cl) is injected into the products of a premixed propane-air flame through four quartz injectors. In a separate experiment we have determined that less than 5% of the ethyl chloride reacts in the injectors before mixing with the hot products. The equivalence ratio, fuel type, and injection amount and temperature can all be varied in these experiments. We have determined that the major products are carbon dioxide, water, HCl, ethylene, and acetylene at temperatures below 1300 K. The concentration of unreacted ethyl chloride is less than 10 ppm, or a destruction efficiency of greater than 99.9%.

ACKNOWLEDGEMENTS

PREFACE

At the end of the engineering education period at L'Ecole Superieure de L'Energie et des Materiaux at University of Orleans, France, a research project has to be performed by the student in order to obtain his Master's Degree. This project is to be done in a company or in a research center and lasts four to six months.

I did this training in Berkeley at the University of California (U.S.A.). My work was performed in the Mechanical Engineering Department with the Combustion Group.

The project dealt with an experimental study of toxic waste incineration. Experiments were conducted in a combustion-driven turbulent flow reactor, burning premixed air and propane. Residence times, temperatures, and equivalence ratios typical of hazardous waste incinerators were attained in the flow reactor. Ethyl chloride was injected downstream of the flame zone, and samples were withdrawn at various points along the reactor. These samples were analyzed using a Fourier Transform Infrared spectrometer coupled with a long path cell.

TABLE OF CONTENTS

LIST OF FIGURES

LIST OF TABLES

9

I. INTRODUCTION:

I.1. OBJECTIVES OF THE STUDY:

The objectives of this study were:

(1) Understanding how operating conditions affect the decomposition of chlorinated compounds.

(2) Develop qualitative and quantitative methods of measuring trace species resulting from combustion using a FT-IR spectrometer coupled with a long path cell.

(3) Simulate and model the conditions of industrial incinerators with respect to residence time and temperature at non ideal conditions.

I.2. TOXIC WASTE INCINERATION IN THE UNITED STATES:

Thermal destruction now accounts for one percent of hazardous waste disposal in the United States, and is an increasingly attractive disposal option. Most hazardous waste combustion research falls into two broad categories:

(1) Understanding and predicting how operating conditions and waste stream composition affect destruction efficiency and formation of undesirable by products.

(2) Developing methods for monitoring the incineration process.

The fist category is of concern because of the desire to maintain a high destruction efficiency, and also because the products of incomplete combustion (PICs) may pose a separate hazard.

Real-time in-situ monitoring is important both for normal process control and for rapid detection of upsets. Permitting for hazardous waste incinerators requires a demonstration of 99.99 percent destruction efficiency for selected waste compounds (Oppelt, 1987). Under well-controlled conditions, destruction rates of hazardous organic substances generally have been observed to be satisfactorily high (Mason et al., 1987).

Fig.1 INCINERATOR OPERATING CONDITIONS

incinerator type	equivalence ratio	T (° C)	residence time (s)
rotary kiln	0.3-0.67	650-1370	1-3
liquid injection	0.3-0.5	700-1650	0.3-2
present experiment	0.3-2.0	500-over 1250	0.3-1.5

source: Oppelt, E.T. (1987). "Incineration of Hazardous Waste," *Journal of the Air Pollution Control Association*, Vol. 37, No.5, pp. 558-586.

Fig.1 presents a chart of the real incinerator operating conditions.

I.3. LOCATION OF RESEARCH:

I.3.1. University of California, Berkeley:

The study of the toxic incineration was performed at Hesse Hall in the Mechanical Engineering Department of the University of California. The experimental apparatus and instrumentation used for this project were available at this location, as was good technical support.

In addition to our project, several other areas of research were being persued in the Mechanical Engineering department, which included the following:

- Lean engine combustion
  The research tasks consisted on: Ignition studies, Heat transfer, Fuel-air mixing/flame propagation, Flame image analysis, Port fuel injection control.

- Turbulent combustion
  Flame spread in an opposed turbulent flow, Micro-gravity combustion, Structure of turbulent diffusion flames.

These projects were conducted by faculty researchers and staff. Graduate and undergraduate students were also involved; most of the graduate students were doctoral candidates.

I.3.2.Lawrence Berkeley Laboratory:

LAWRENCE BERKELEY LABORATORY is a multinational laboratory managed by the University of California for the U.S. Department of Energy (L.B.L. research review Vol.14 spring 1989). The oldest of the nine national laboratories, LBL is the only one located next to one of the famous universities of the United States, the University of California, Berkeley.

Fig.2 LAWRENCE BERKELEY LABORATORY
UNIVERSITY OF CALIFORNIA

```
                        ┌──────────────┐
                        │  DIRECTOR'S  │
                        │  COMMITTEE   │
                        └──────────────┘
┌──────────────────┐                      ┌──────────────────┐
│  ADMINISTRATION  │                      │     PLANNING     │
│                  │                      │       AND        │
│                  │                      │   DEVELOPMENT    │
└──────────────────┘                      └──────────────────┘

┌──────────────┐      ┌──────────────┐      ┌──────────────┐
│    ENERGY    │      │   GENERAL    │      │     LIFE     │
│   SCIENCES   │      │   SCIENCES   │      │   SCIENCES   │
└──────────────┘      └──────────────┘      └──────────────┘

┌──────────────┐      ┌──────────────┐      ┌──────────────┐
│   APPLIED    │      │  ACCELERATOR │      │   RESEARCH   │
│   SCIENCE    │      │   AND FUSION │      │   MEDECINE   │
│   DIVISION   │      │ RESEARCH DIV.│      │  BIOPHYSICS  │
└──────────────┘      └──────────────┘      └──────────────┘

┌──────────────┐      ┌──────────────┐      ┌──────────────┐
│ EARTH SCIENCE│      │   NUCLEAR    │      │   CELL AND   │
│              │      │   SCIENCE    │      │   MOLECULAR  │
│   DIVISION   │      │   DIVISION   │      │ BIOLOGY DIV. │
└──────────────┘      └──────────────┘      └──────────────┘

┌──────────────┐      ┌──────────────┐      ┌──────────────┐
│ MATERIALS AND│      │   PHYSICS    │      │   CHEMICAL   │
│   CHEMICAL   │      │              │      │ BIODYNAMICS  │
│ SCIENCE DIV. │      │   DIVISION   │      │   DIVISION   │
└──────────────┘      └──────────────┘      └──────────────┘

┌──────────────┐      ┌──────────────┐      ┌──────────────┐
│  ENGINEERING │      │  INFORMATION │      │ OCCUPATIONAL │
│              │      │   COMPUTING  │      │              │
│   DIVISION   │      │ SCIENCES DIV.│      │  HEALTH DIV. │
└──────────────┘      └──────────────┘      └──────────────┘
```

13

In 1989, LAWRENCE BERKELEY LABORATORY had more than 3,000 employees. Its total budget of about $200 million supports a wide range of research activities in fields ranging from astrophysics to energy conservation.
The Laboratory's rule is to serve the nation and its scientific and educational communities through energy-related research performed in its unique facilities.
LBL's role forms a four part mission:

- to perform leading multidisciplinary research in energy sciences.
- to develop and operate unique national experimental facilities for use by qualified investigators
- to educate and train future generations of scientists and engineers.
- to foster productive relationships between LBL research programs and industry.

Current programs encompass all the natural sciences, as well as engineering, mathematics, and computer sciences. Basic studies of the atom and the cell, research on new treatments for cancer patients , and the development of advanced materials instruments, facilities, and new energy sources are typical examples of LBL research.

Fig.2 presents an organization diagram of the different L.B.L. Departments.

I.3.3. The research group:

Six people were involved in this research project: Dr. Donald Lucas (my supervisor), Staff Scientist at Lawrence Berkeley Laboratory, Professor Catherine P. Koshland from the Biomedical and Environmental Health Department, Professor Robert F. Sawyer and Elisabeth Fisher, graduate student, from the Mechanical Engineering Department of U.C.Berkeley, Dr. Matthew J. Hall, Staff Researcher at U.C.B., and myself, a visiting researcher in the L.B.L. Applied Science Division.

II. EXPERIMENTAL APPARATUS:

II.1. DESCRIPTION OF THE EXPERIMENT:

Our experiments were conducted in a combustion driven flow reactor burning a premixed air-propane mixture. Ethyl chloride was injected down steam of the flame and samples were withdrawn at various points along the reactor. Measurements of temperature and species concentrations at intervals along the reactor allowed us to determine the time history of the destruction process. These samples were analyzed with an FT-IR spectrometer and with an exhaust analyzer.

Fig.3 illustrates the whole experimental set up.

II.2. FLOW REACTOR SETUP:

The combustion tunnel consists of a combustion section, a chlorinated hydrocarbon injection region, and a reaction and sampling section.

II.2.1. Tunnel characteristics:

The tunnel was constructed of stainless steel and had a circular cross-section with an inside diameter of 5.1 cm. Stable and reproducible burning of the fuel /air mixture was accomplished in the first section. Air was supplied by a laboratory compressor at a maximum pressure of 90 PSI. All reactant flow rates were measured by rotameters calibrated with the appropriate fluid and were corrected for temperature and pressure variations. The tunnel pressure was near atmospheric. Ports in the walls of the tunnel allowed gas samples to be withdrawn and thermocouples to be inserted.

The reaction and sampling region began immediately downstream the flame. This four meter section was insulated with layers of 2.5 cm thick Fiberfrax alumina silica insulation (ceramic fiber) to reduce heat losses and to minimize radial and axial temperature gradients. Water manometers were installed upstream and 4 meter downstream from the flame to determine pressure differences inside the tunnel.

15

FLOW REACTOR

PROPANE

AIR →

Flame holder   Ignitor   Cooling Air   Ethyl chloride injection   P

T   P   T T   T   T   T   T

|Mixing section| Combustion section|————Reaction and sampling section————|

EXHAUST →

SAMPLING MANIFOLD

Heat taped sample lines

Exhaust ← Vacuum Pump

Vacuum Manifold →

Exhaust ← Vacuum Pump

CELL

Detector   I.R. Source

FTIR INTRUMENT

Cold trap →

CO (low)
CO (high)
NO
CO2
O2
CxHy

→ Exhaust

GAS ANALYSIS SYSTEM

Fig.3
EXPERIMENTAL SETUP

The reactor was ignited by a spark located in the combustion section.

A pressure relieve diaphragm was mounted upstream of the mixing section to guard against a sudden over pressurization.

Different tunnel configurations could be chosen, as the sections of the tunnel were interchangeable. Special sections included a transparent quartz section located at the end of the combustion section (which allowed visual inspection of the flame), a gaseous fuel injection manifold, a flame holder section, a spray nozzle for injection of liquid fuels, a 10.2 cm diameter section of steel tubing (to increase the residence time of the reactants in the flame region), and a manifold for the injection of gaseous chlorinated hydrocarbons.

II.2.2. Air and fuel system:

Air for the tunnel was supplied by an air compressor and was regulated by a mass flow controller having a capacity of 500 lpm. When premixed combustion was desired, propane was injected into the air stream at four locations around the circumference of the tunnel: mixing was accomplished with baffles and the mixture was burned at a flame holder which consisted of a screen in the tunnel cross-section. A mass flow controller similar to the one used for the air was installed to control the propane flow. The pressure upstream of the mass flow controller was maintained at 60 PSI.

Non-premixed liquid spray combustion could also be studied. A nitrogen pressurized liquid fuel reservoir supplied heptane to a spray nozzle section which could be inserted into the tunnel in place of the flame holder section. The spray nozzle had a single hole and produces a finely atomized hollow-cone spray. The nozzle was located on the axis of the tunnel, and the spray was directed downstream. The spray nozzles were interchangeable to give different flow rates and spray angles. The minimum operating pressure to ensure proper atomization for the different nozzles was 60 PSI. Preliminary investigations have begun to determine the approximate droplet size distributions using a microscope to examine droplets collected on glass slides.

17

II.2.3. Range of equivalence ratios:

We were able to operate the combustor over a wide range of equivalence ratios. For the propane-air flame we were able to vary phi between 0.55 and 1.1. The lean flammability limit was about 0.55 at an air flow rate equal to 5.2 gps. The flammability limits for propane/air mixtures restrict the equivalence ratio to between 0.52 and 2.45 (Weast et al., 1983).

The equivalence ratios were not in the same range as the typical equivalence ratios of industrial practice, because the industrial incinerators generally burn liquid or solid fuel and operate at high excess air, resulting in a low equivalence ratio. Our device couldnot attain such low equivalence ratios when it burned premixed air and gaseous fuel.

II.2.4. Cooling systems:

The temperature of the combustion products leaving the first section was adjusted by watercooling of the tunnel wall. 22.5 m of 0.6 cm copper tubing was wrapped around the 10 cm diameter section of the tunnel. Water flow rates up to 4 lpm through the tubing permits adjustment of the gas temperature by nearly 100C.

Also, air injection down stream of the flame was possible, using a section having four symmetrically located steel injectors. The air flow rates range was between 1 to 3 gps.

II.2.5. Chlorinated species injection:

A system to inject gaseous chlorinated hydrocarbons was installed. It was used to inject ethyl chloride and methyl chloride into the test section at rates of approximately 0.5% of the total mass flow without the air dilution added for cooling. Ethyl chloride (C_2H_5Cl) was selected as the first species for injection because it contains chlorine while being relatively non-toxic. The flow rate was controlled by a mass flow controller located downstream of the gas bottle. Ethyl chloride has a low vapor pressure and must be heated to obtain sufficient pressure for the flow controller to operate properly; the line upstream the mass flow controller was also heated to prevent condensation in it.

18

Fig.4 SCHEMATIC DIAGRAM OF THE INJECTORS

SWAGELOCK
FITTING

COMBUSTOR
WALL

3.18 mm

19.1 mm

FIBERFRAX
INSULATION
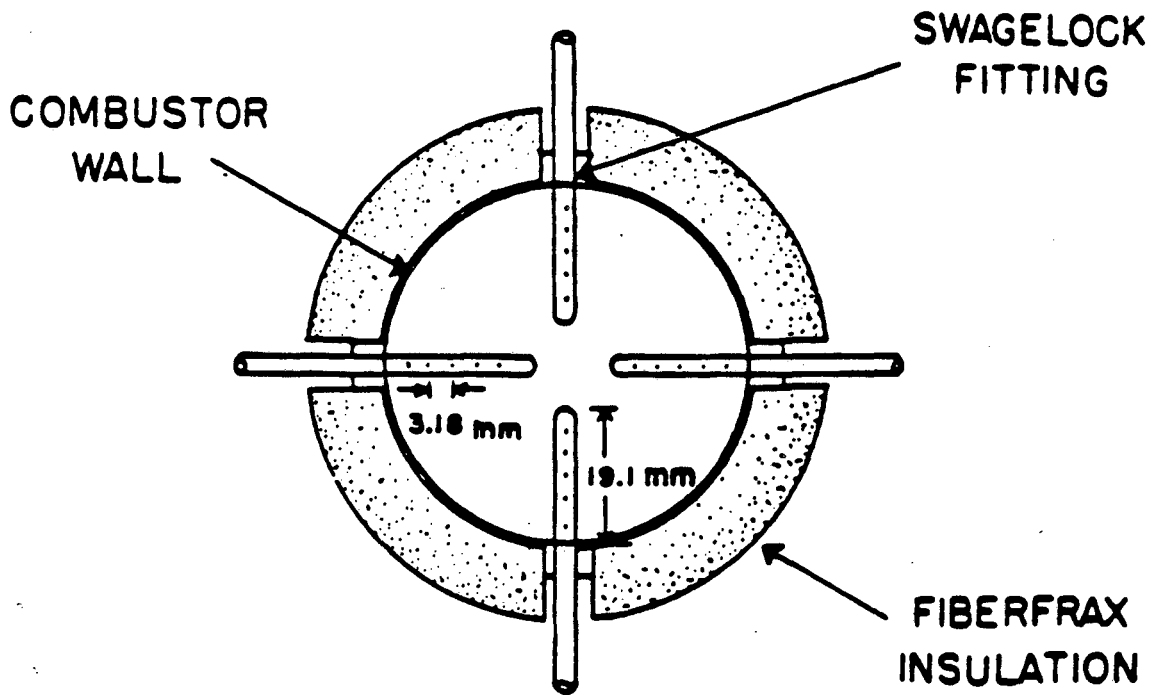
QUARTZ INJECTORS

3.0 mm outside diameter
2.0 mm inside diameter
0.4 mm hole diameter

19

The gaseous chlorinated compounds were introduced into the product gas stream through four symmetrically oriented quartz injectors, shown schematically in **Fig.4.** The injectors were positioned to supply the ethyl chloride counter-flow to the combustion product stream, which aids in rapid mixing.

Tests on the ethyl chloride decomposition inside the quartz probe were performed. Ethyl chloride flowed through a long (10cm) quartz tube placed across the tunnel section. Appropriate flow rates were chosen in order to simulate the injection condition with respect to residence time and temperatures. Less than 0.1 % of the ethyl chloride decomposed under these conditions.

II.3. MEASUREMENT TECHNIQUES:

II.3.1. Temperature measurement:

Eight bare Chromel/Alumel (type k) thermocouples were used to measure temperatures along the tunnel at different axial locations. The thermocouples were positioned at a desired radial location by inserting stops in port on the tunnel wall. The uncertainty in the radial position using this method was estimated to ± 2 % of the diameter. Although, all the thermocouples were centered inside the tunnel, for most of the measurement the drawback of that operation was that the combustor had to cool down to be able to modify their position.

TABLE I.

Location of the thermocouple in the flow reactor burning a propane-air mixture for a specific tunnel configuration.

A: Labels of the thermocouples
B: Distance of the thermocouple from the flame holder.
C: Transit time for plug flow to the thermocouple location at a total stoichiometric flow rate of 5.5 gps air-propane mixture and a mean tunnel temperature of 1000K.

A	B	C
2.	78.0 cm	55.0 ms
3.	103.5 cm	74.0 ms
4.	164.5 cm	117.5 ms
5.	177.0 cm	126.4 ms
6.	277.0 cm	198.0 ms
7.	226.0 cm	161.0 ms
8.	394.5 cm	282.0 ms

II.3.2. Sample extraction:

Gas samples were withdrawn from the reaction section through stainless steel probes having a 3.2 mm inside diameter to a sample manifold. The manifold consisted of seven inlet valves used to select the desired sample line, and two outlet valves, one connected to a heat taped line going to the FT-IR spectrometer and one going to the exhaust gas analyzer.

TABLE II.

Location of the sample lines in the same tunnel configuration described previously:

A	B	C
1.	78.0 cm	55. ms
2.	96.5 cm	68. ms
3.	103.5 cm	129. ms
4.	191.5 cm	135. ms
5.	123.7 cm	87. ms
6.	251.5 cm	177. ms
7.	351.5 cm	276. ms

A: Labels of the sample lines.
B: Distance from the flame holder.
C: Transit time for plug flow to the sample line, for similar burning condition as described for the thermocouple location.

II.3.3. Data acquisition:

A PC compatible computer was installed for data acquisition and processing. An analog to digital converter was used to collect, display, and store the temperatures measured at seven locations along the axis of the tunnel. An additional computer board was used to measure the signals from the exhaust analyser.

II.4. ANALYSIS TECHNIQUES:

Combustion gases withdrawn from the tunnel were analyzed with two instruments, a Fourier Transform Infrared spectrometer, which was our major tool of investigation, and an exhaust gas analyzer.

II.4.1. The exhaust analyzer:

Carbon dioxide and carbon monoxide were measured using Horiba nondispersive infrared (NDIR) continuous gas analyzers. Concentration of oxygen was determined by a Beckman Model 315 gas analyzer. A Horiba flame ionization analyzer measured unburned hydrocarbons. Metal bellows vacuum pumps, located in the analyzer housings, were used to withdraw the samples. Unheated stainless lines were used to transport the gases to the analyzers. Water was removed through the use of two ice-bath cooled condensers in series.

II.4.2. Fourier Transform Infrared Spectroscopy:

II.4.2.1. Spectroscopy overview:

Spectroscopy can be used to determine the identity, the structure, and the environment of atoms and molecules by analysis of the radiation absorbed by them. The energy that atoms and molecules can possess, according to quantum theory, is quantized. That is, in an atom or molecule, energy can have only certain discrete values. The allowed energies are called atomic or molecular energy levels. The energy of an atom or molecule is made up of translational, rotational, vibrational, and electronic energy.

Translational energy is the kinetic energy atoms or molecules possess due to motion in space. Quantum

restrictions are not important in this case, because all the energy levels are so close that they form a continuum.

Rotational energy is the kinetic energy molecules possess due to rotation about an axis through their center of mass. Rotational energy is quantized and gives rise to absorption spectra in the infrared region of the electromagnetic spectrum. The difference between rotational energy levels is inversely proportional to the moment of inertia (I) of the molecule.

$$\delta E \ \alpha \ 1/I$$

$$I = \mu * r^2$$

where $\mu = \dfrac{m_1 * m_2}{m_1 + m_2}$ is the reduced mass and r is the separation between masses m_1 and m_2.

Vibrational energy is the potential and kinetic energy molecules possess due to vibrational motion. Vibrational energy is also quantized and the relative spacing between energy levels increases with increasing strength of the chemical bond between atoms.

The infrared spectrum of a molecule is a result of transitions between two different vibrational energy levels, which means an atom or molecule is excited to a higher energy level by absorption of a photon. The vibrational frequency of a chemical bond is a function of the bond strength and the reduced mass.

$$v = \frac{1}{2\pi} (k/\mu)^{1/2}$$

$$E_2 - E_1 = hv$$
$$E_2 - E_1 = \text{Transition energy}$$

23

Each different kind of atom or molecule has its own characteristic absorption spectrum. Each line or band is characteristic of a particular molecular bond, and once the characteristic line pattern of a species is known its appearance in the spectrum establishes the presence of that species in the sample. It is made quantitative by measuring absorptions as well as wavelengths.

Vibrational modes are infrared active under the following conditions:

- the requirement for infrared activity of a vibration is that the vibration must produce a change in the dipole moment. The symmetry of a molecule determines if there is a change in the dipole moment, and, consequently, if a characteristic frequency is possible.

- the intensity of the vibration must be large enough to make the vibration observable in the presence of other molecular vibrations.

II.4.2.2. Spectrometer:

The FT-IR spectrometer used for this experiments was a Digilab FTS-40 spectrometer with a cooled Mercury Cadmium Telluride (MCT) detector, coupled with a multi-path cell from Infrared Analysis Inc., fitted with ZnSe windows.

II.4.2.2.1. Instrument principle:

The main part of the FT-IR spectrometer is an optical bench containing an infrared radiation source which is phase modulated by a Michelson interferometer and passed through a long path cell containing the sample to be analyzed. The transmitted radiation is measured with a cooled detector, and the data are recorded and stored. See Fig.5. A Fourier transform is performed on the data to obtain absorption spectrum. Background subtraction is used to eliminate contaminants and normalize for the instrument function. Liquid nitrogen is used to supply gas to purge the optical bench of water and carbon dioxide, and to support the air bearings of the Michelson interferometer.

The instrument is equipped with a Motorola 68,000 microprocessor, with a hardware Fourier transform board, and a RAM memory of 5.12 kbytes. Software is available for manipulating and displaying the spectra. The ability to add
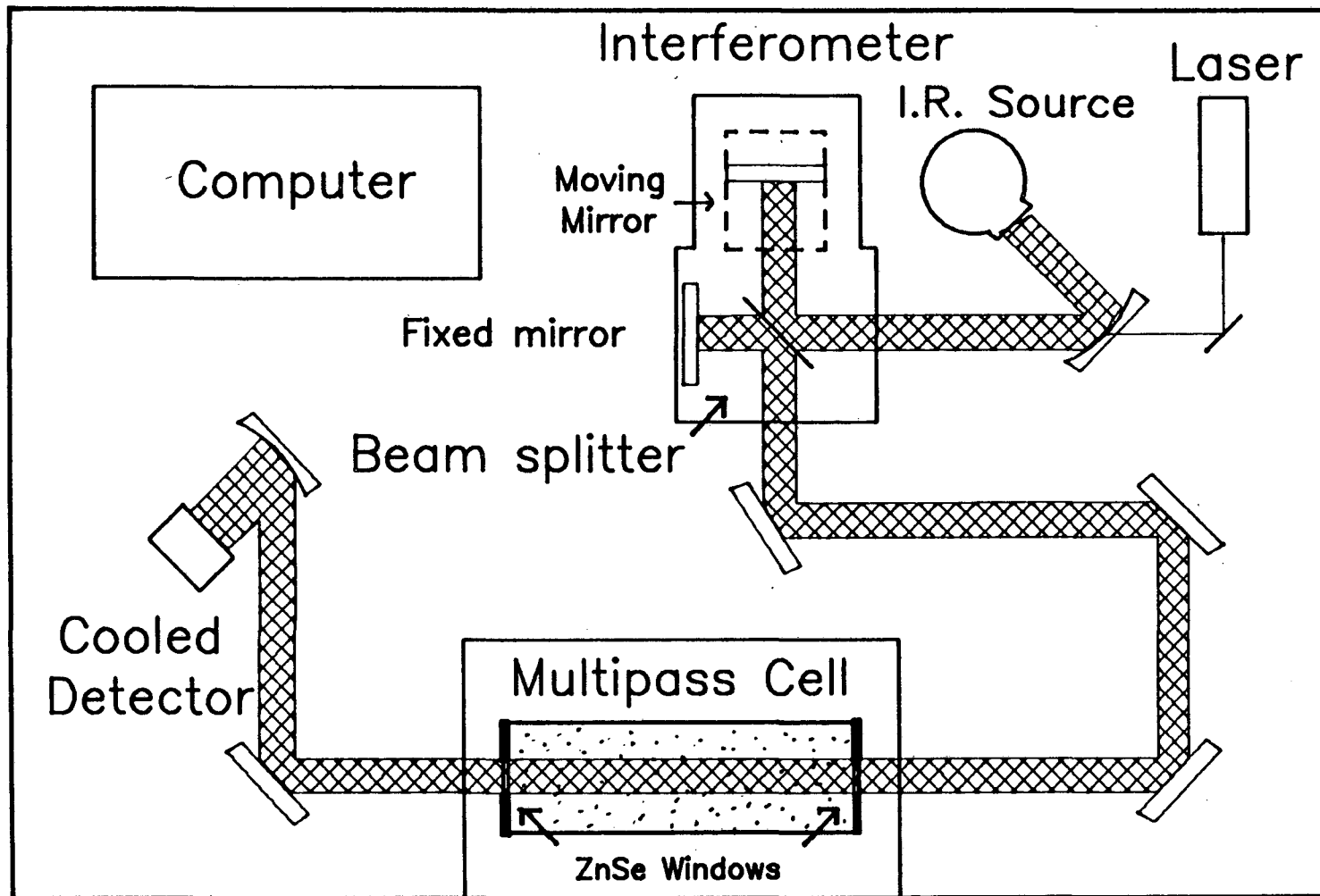
24

FT-IR SPECTROMETER

Fig.5 Schematic of an FT-IR

and subtract spectra in digital form is specially useful in eliminating interferences due to overlapping bands, allowing us to extract the maximum amount of the information from the spectra.

II.4.2.2.2. Characteristics:

Mirror displacement:

The mirror displacement of the Michelson interferometer is measured by counting the number of the interference fringes formed by a HeNe laser providing an accurate positioning information.

The interferogram $I(x)$ of a monochromatic source, emitting at the frequency v (cm^{-1}) is given by

$$I(x) = A \cos 2\pi vx$$

where x is the optical retardation (in centimeters) and A is the amplitude factor. We can see that, for a stable monochromatic source, zeros in the interferogram are well defined and occur at optical retardations which are multiples of the emission frequency; therefore, this is a good internal measure of the mirror position. See Fig. below.
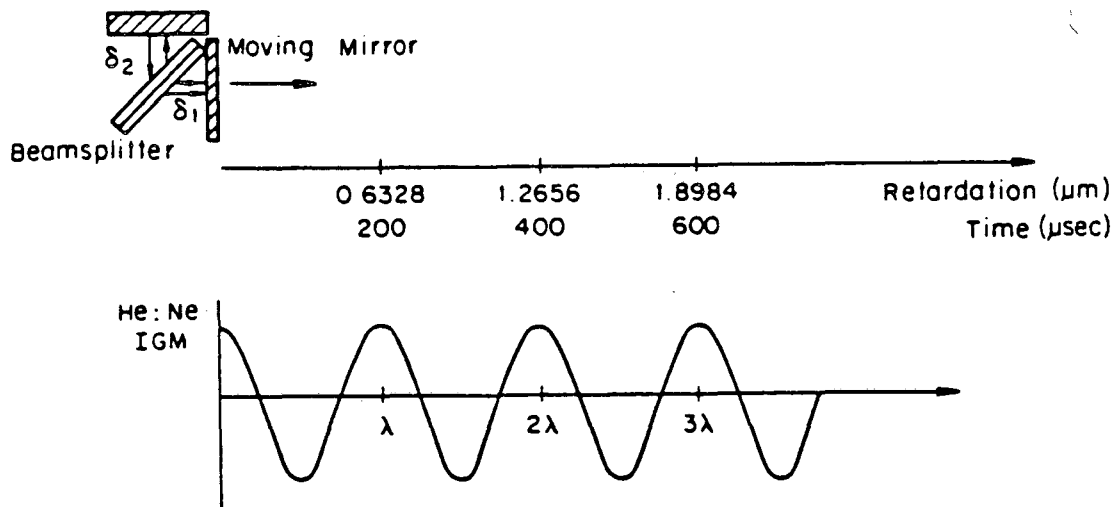
Rapid scan:

For a Michelson interferometer it has been shown that (see, e.g., Griffiths, 1975), to first order, the moving mirror maximum displacement from the point of zero optical retardation, δx, is related to the resolution δv by

$$\delta x \, \alpha \, 1/\delta v$$

In case the interferogram is to be obtained in time δt, the moving mirror must have a velocity V is given by

$$V = 1/2(\delta x/\delta t)$$

Further more, continuous scanning interferometer systems require electronic filtering in the signal chain, where the filter bandpass is matched to the moving mirror velocity, since the electrical frequency f for a particular optical frequency v is given by

$$f = 2Vv$$

Resolution:

"Resolving" can mean, according to authors, the presence of a 100 % dip between the lines (digilab cretierion), or a 20 % dip (Raleigh criterion), or the first detectable distortion from the peak due to single line (Hirschfeld, 1964; Jacobi, 1968).

In order to obtain the full amount of information available in the spectrum, the instrumental resolving power must be sufficient to permit the recording of the true shapes of the spectral lines and the fine structure of the molecular bands.

The required resolution is a function of the total pressure in the cell due to the effect of the pressure broadening and the linewidth of the trasition being probed.

On the instrument level, the resolution of the FT-IR spectrometer is defined as the inverse of the length of mirror travel beyond the zero path difference, which is expressed in reciprocal centimeters (cm^{-1}) or wave numbers.

Using high resolutions increase the analysis time and data storage requirements, for an appreciable gain in the

signal-to-noise level. Optimum resolution would provide adequate specificity with an appropriate balance between signal-to-noise and analysis time. An adequate compromise had to be found between;

(1) analysis time
(2) signal-to-noise ratio
(4) ability to differentiate compounds with overlapping spectra
(5) data storage (size of the spectra).

Apodization function:

Two apodizations functions could be used, the boxcar or the triangular function. These are the square (or Boxcar) function, producing a (sin x/x) spectral slit profile, and the triangular function peaking where the interferogram does, producing a $(sin^2 x/x^2)$ spectral slit profile. A paper (Chantry and Fleming, 1976) showed that, boxcar apodization gave $0.66/\delta_{max}$ cm^{-1} resolution, while triangular apodization gave $0.83/\delta_{max}$ cm^{-1} resolution, a 25 % loss.(δ is the retardation in cm^{-1} corresponding to the travel of the moving mirror). Also the boxcar apodization function was found to be more accurate, and maintained its accuracy to far higher absorbances, than the triangular apodization function.

For all our experiments the boxcar apodization function was used.

Long path cell:

White Optical System, Basic Four Passes

28
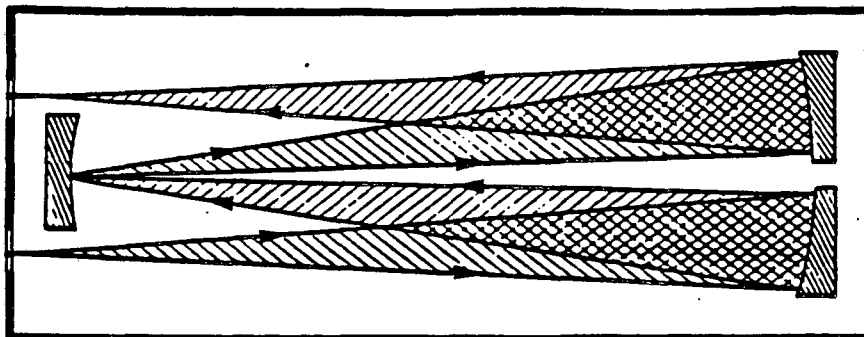
The samples were collected in a long path cell through which the infrared beam was passed. The beam was reflected by a three mirror system which gave multiple-pases in increments of 4 passes. See previous Fig. The pathlengths are variable from 2.2 meters to more than 28 meters. The system includes two vacuum valves, a pressure release valve, a vacuum gauge, provision for gas flow-through, silver coated mirrors, and a six mirror transfer optics system that coupled the long path cell to the FT-IR spectrometer.

The only major source of energy loss in the system was the absorption at the mirror surfaces. If R is the reflectivity of the mirrors, the fraction of the input energy which will be lost at n reflections will be $(1-R)^n$. The long path cell has measured throughputs of between 20 to 95 % of the signal for different passes.
A helium-neon laser was used for alignment.

Detectability limits:

It can be assumed that we can detect any spectral line or band which is approximately as strong as the noise level in the spectrum. The noise level is a function of the source intensity, the number of scans, the spectral resolution, the type of optical filters used, the stability of the optical components, and other operational factors. The path length for maximum signal-to-noise level is function of the mirror refletivity. The detection limit for a weak absorption will be improved by increasing the path length and degraded by reflection losses. The optimum conditions in the multiple pass cell were found experimentally for each species.

29

III. METHOD OF APPROACH:

III.1. Instrument calibration:

Both flow meters used for propane and for ethyl chloride injection, were calibrated using a Brooks Vol-U-Meter flowmeter having a volume of 3.5 l. The seal between the piston and the glass cylinder is formed by mercury o-ring which permits essentially frictionless movement of the piston. This instrument consists of a hermetically sealed piston which moves in a precision bore, borosilicate glass cylinder. By observing the displacement of the piston and measuring the time interval for this displacement, the volume per unit time is determined. A detachable scale calibrated in cubic centimeters is mounted adjacent to the glass cylinder. Corrections for temperature and pressure were performed.

Pressure gauges were calibrated using a classical mercury manometer, except the gauge used in the sample manifold which read low pressure (0.5 to 20 torr). This was calibrated with a McLeod gauge consisting on a mercury manometer based on the compression of a fixed amount of confined gas.

The air flow meter, because of its high capacity (500lpm) flow rate, was calibrated with an air displacement bell flow meter having a volume of 5 ft^3.

Calibration curves presenting the behavior of all the instruments are presented in **Fig.26 to 30**.

III.2. Measurements on the combustor:

III.2.1. Fluid dynamic characteristics:

A fixed flow rate of air (5.2 gps) was used for all the experiments run in the tunnel.

The Reynolds number is given by :

$$Re = \frac{V.D}{v}$$

Where: V is the velocity in m/s
D is the section diameter in meters
v is the kinematic viscosity in m^2/s

$$V = Q/S; \quad S = 19.64 cm^2 \text{ is the tunnel section}$$

For a stoichiometric propane/air mixture, assuming ideal gas behavior, we calculated that the Reynolds number varied between 2500 and 6000 for a mean temperature along the tunnel between 800 and 1300 K.

For a propane/air flow rate Q equal to 6.9 lps (air+propane), at room temperature v is equal to 16.8×10^{-6} m^2/s, and at 1200K, v is equal to 159.1×10^{-6} m^2/s. **Table III** shows values of the Reynolds number, velocity and residence time for different mean temperatures of the tunnel.

Because of the strong temperature dependency of the dynamic viscosity, the Reynolds number increased by a factor of two or more as the gases passed through the combustor.

At this range of flow rate, the combustion was turbulent and an adequate residence time for the injected chlorinated species was obtained.

TABLE III.

Fluid dynamic characteristics

Temperature	Reynolds number	Velocity	Residence time[*]
398K	10500	3.5 m/s	860 ms
1000K	5000	11.7 m/s	260 ms
1200K	4400	14.0 m/s	210 ms

[*] Residence time is the transit time calculated for plug flow over 2.77 meters in the tunnel.

III.2.2. Temperature characteristics:

III.2.2.1. Axial temperature profile:

Axial temperature profiles for a propane/air mixture at different equivalence ratios is shown in Fig.6. The initial temperatures for X=0, representing the temperature of the flame are the calculated adiabatic flame temperatures. They were calculated using "STANJAN--Interactive Computer Programs for Chemical Equilibrium Analysis" (Stanford, CA 94305, 1981). A significant drop of temperature, at all equivalence ratios, is noted for distances between 5 and 75 cm where the tunnel is not insulated. In all cases, there is more than 300 degrees Celcius temperature gradient.

III.2.2.2. Radial temperature profile:

Radial temperature variations were measured at different radial position known within 2 mm. Radial temperature profiles measured at 78 and 277 cm downstream the flame holder are shown in Fig.7. The curves present temperature of one thermocouple located downstream of the flame in the non-insulated portion of the tunnel and one located in the sampling area which is insulated. The tunnel was operating with a propane/air mixture at an equivalence ratio of 0.9.

The temperature gradient K/cm in the non-insulated section is 140 while in the insulated section the gradient is equal to 40 K/cm.

III.2.2.3. Range of temperatures in the flow reactor using air dilution:

To achieve lower temperatures in the tunnel, a lean propane/air mixture was burned. To maintain steady combustion the equivalence ratio was fixed at a minimum of 0.63. Diluting air was added down stream (75cm from the flame holder) to further reduce tunnel temperatures when desired. Fig.8 shows the variation of the temperature at different air flow rates for each thermocouple location.

III.2.2.4. Evolution of the tunnel temperature after ignition:

We had to ignite the combustor one hour before analyzing

Fig.6

Axial temperature profile for various equivalence ratios

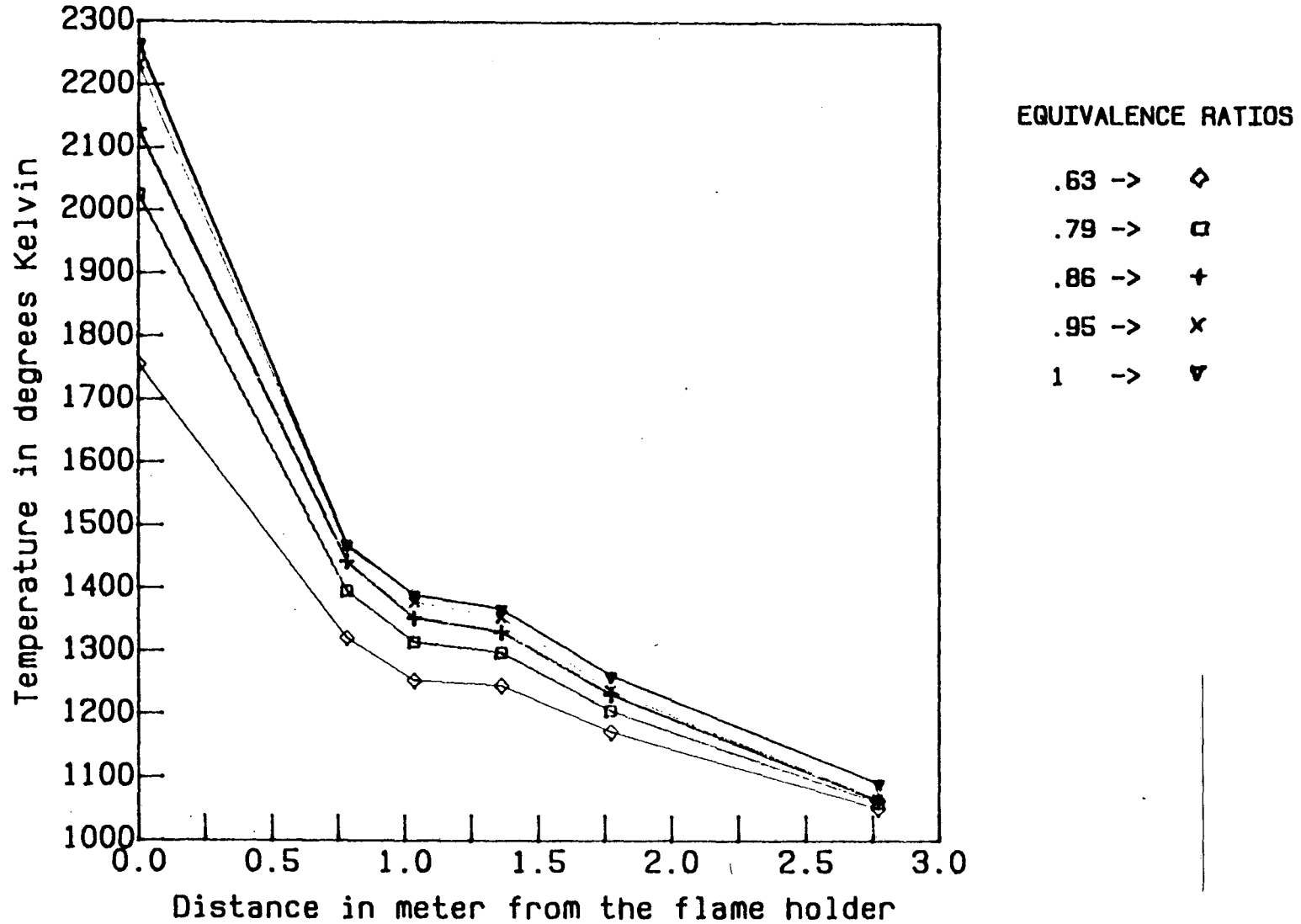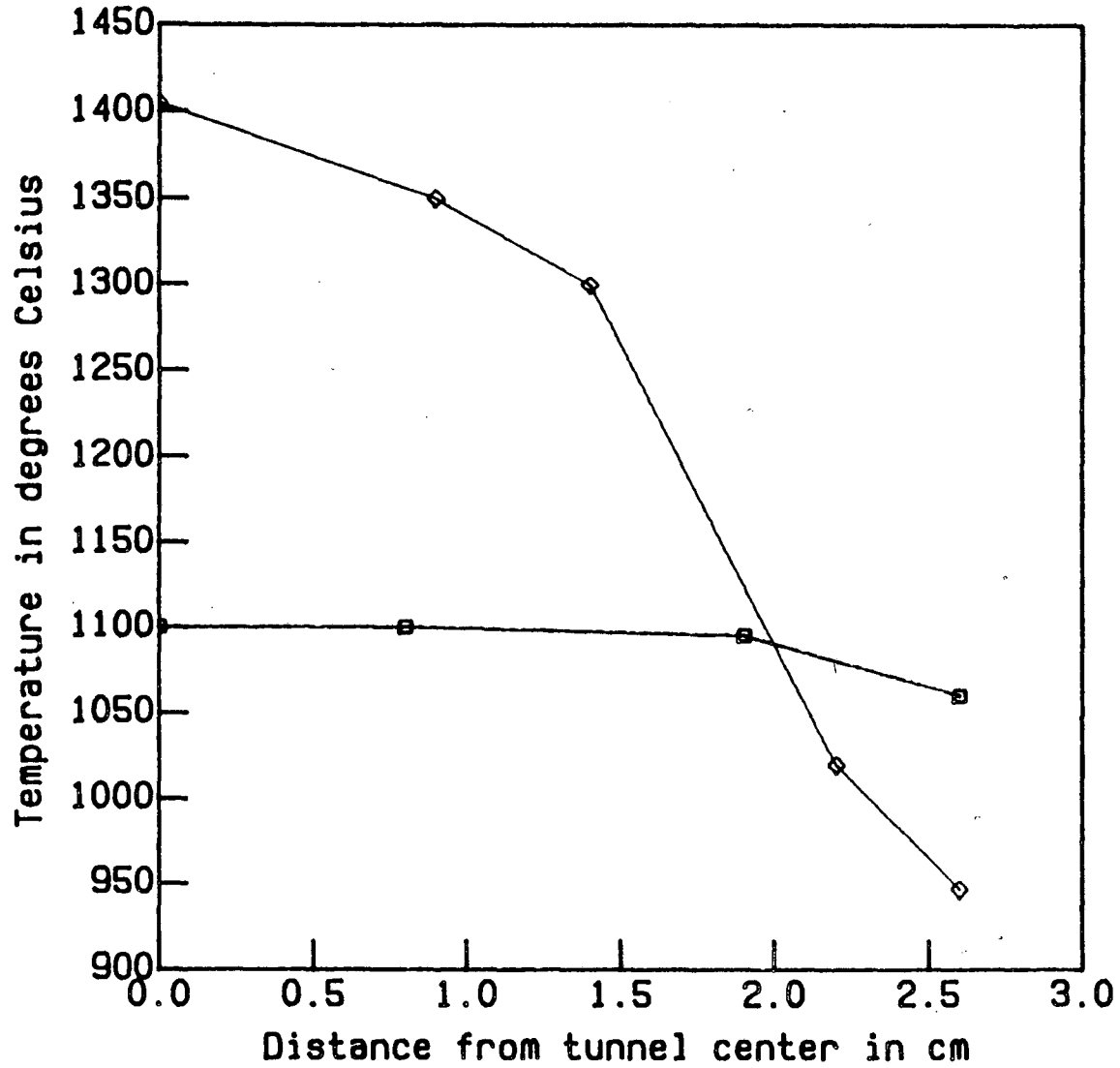Tunnel configuration: All section diameters=5.1 cm;

Fig.7

RADIAL TEMPERATURE PROFILE at Φ̄=0.9

Tunnel configuration: All section diameters=5.1 cm;
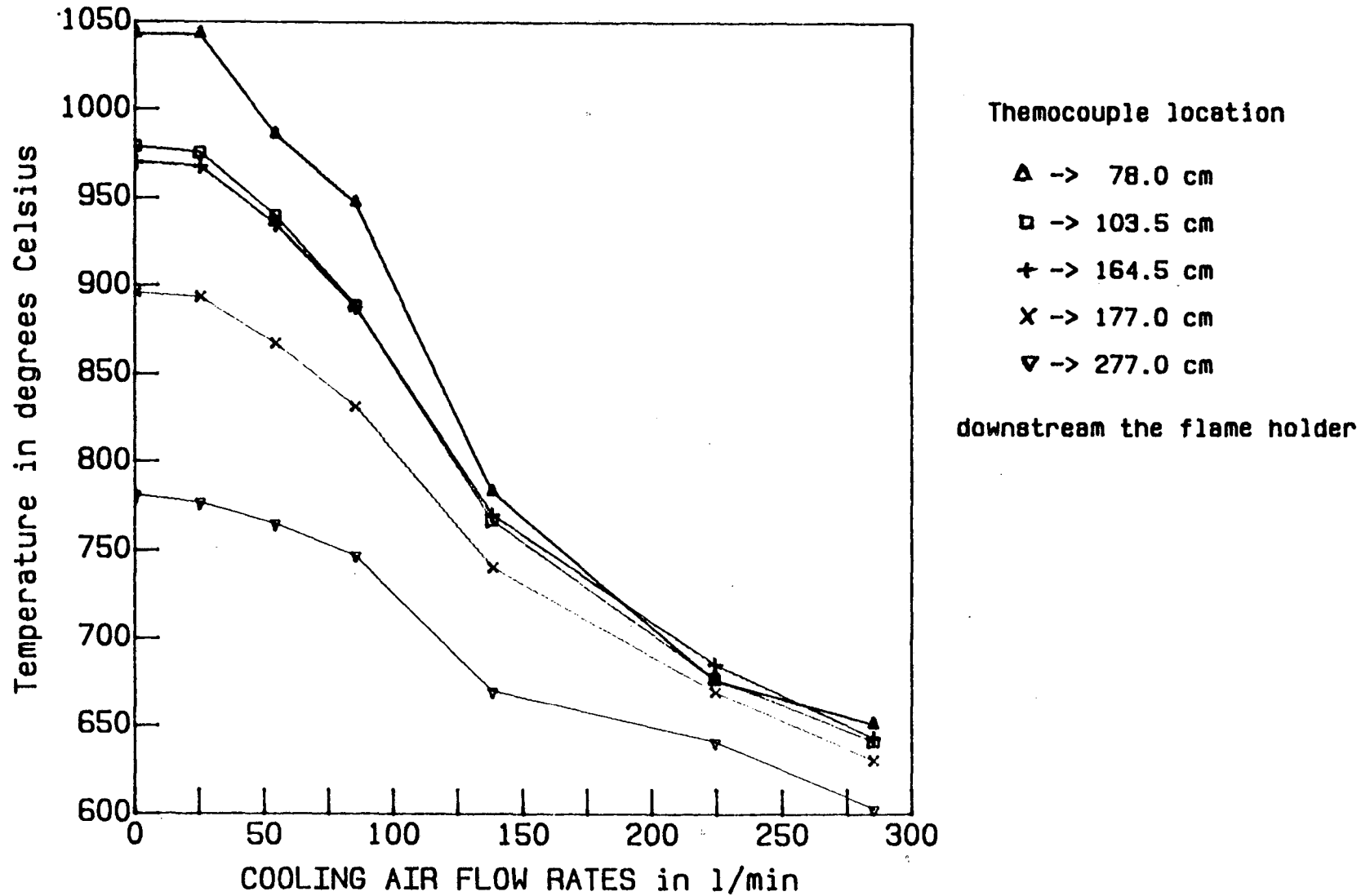
Thermocouple locations:

78 cm -> ◇

non insulated section

277 cm -> ◻

insulated section

Fig.8

Thermocouple temperature with various cooling air flow rates

Tunnel configuration: All section diameters=5.1 cm; Phi=.63

Thermocouple location

△ -> 78.0 cm

◻ -> 103.5 cm

+ -> 164.5 cm

✗ -> 177.0 cm

▽ -> 277.0 cm

downstream the flame holder

species withdrawn from the tunnel. This was the minimum time to heat up the tunnel, in order to obtain constant temperature.

Fig.9 gives an indication of the temporal increase of temperature for each thermocouple under some conditions.

III.3. Calibration and effects of different parameters on the reference samples:

III.3.1. Method of measuring low concentrations:

Three different procedures were developed to measure species at the low concentrations needed as references.

The first relies on a 0-20 torr pressure gauge. The sample manifold was filled with the desired species to a fixed pressure,(usually less than 10 torr). The cell was evacuated to approximately 20 millitorr. By opening the valve connecting the manifold to the cell, the sample expanded by a factor of 10.77, which represents the volume ratio of the cell versus the manifold ratio. The drawback of this procedure is that the residual gas at ~20 millitorr in the cell, becomes important when the pressure is below a tenth of a torr.
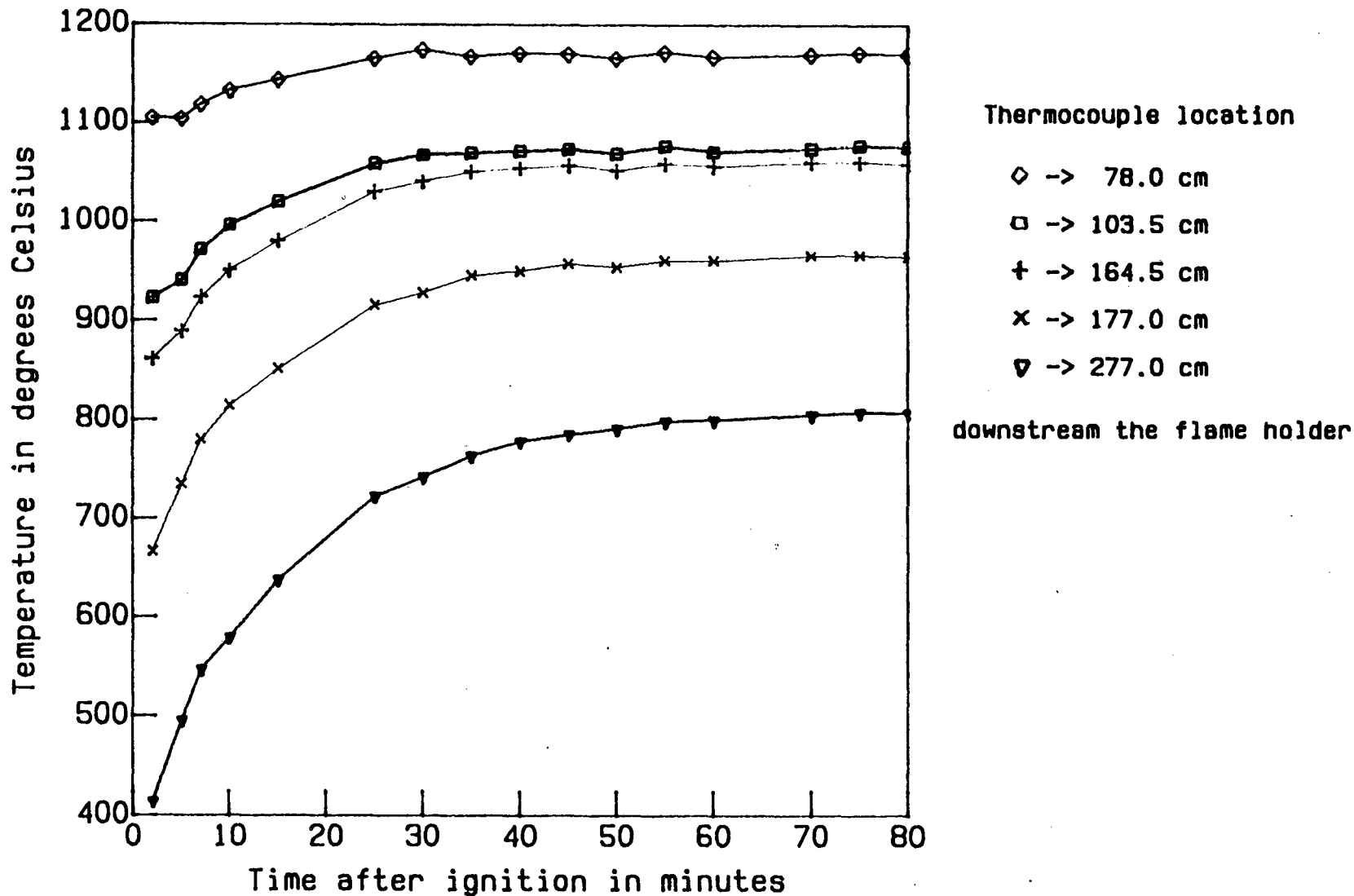
The second method was based on a dilution of the calibration species with nitrogen. It consisted of filling the sample manifold and the cell with the desired species at a fixed pressure, usually less than 20 torr, then adding nitrogen to one atmosphere. The mixture was partially evacuated from the cell to achieve the desired concentration. Although this method allowed us to measure concentration below ppm levels with 10% uncertainty, to ensure homogeneous mixing and proportional evacuation of the mixture, experiments proved that we needed to wait more than 30 minutes before evacuating the cell. Lower concentrations were achievable using this method.

The last method used gas tight syringes having volumes of 0.5cc and 10cc. The volume of the cell was determined to be equal to 4830 cc ± 0.5%, by expansion of a known volume of gas, and also by using a Brooks Vol-U-Meter. The species were injected into a nitrogen stream flowing into the previously evacuated cell. This method was chosen for calibration of most species because it had the smallest

Fig.9

Temperature evolution after combustor ignition

with a propane/air mixture for Phi=.86

Thermocouple location

◇ -> 78.0 cm

▫ -> 103.5 cm

+ -> 164.5 cm

✕ -> 177.0 cm

▽ -> 277.0 cm

downstream the flame holder

uncertainty. In addition, it was faster than the other methods, especially, for the low concentrations since it avoided multiple dilutions and the long mixing times.

The three procedures were found to agree within 3%, for the same range of concentrations.

III.3.2. Effect of the optical density on the absorbance:

The Beer-Lambert law states that the absorbance is given by:

$$A = \alpha.c.l.$$

path length
concentration
absorption coef.
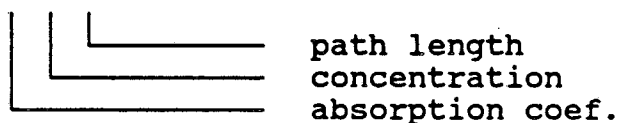
It predicts a linear relationship between the concentration path length product and absorbance.

Varying the optical density, which represents the product of the concentration times the path length, showed species had different behavior with respect to absorbance. See **Fig.10** which present the calibration system.
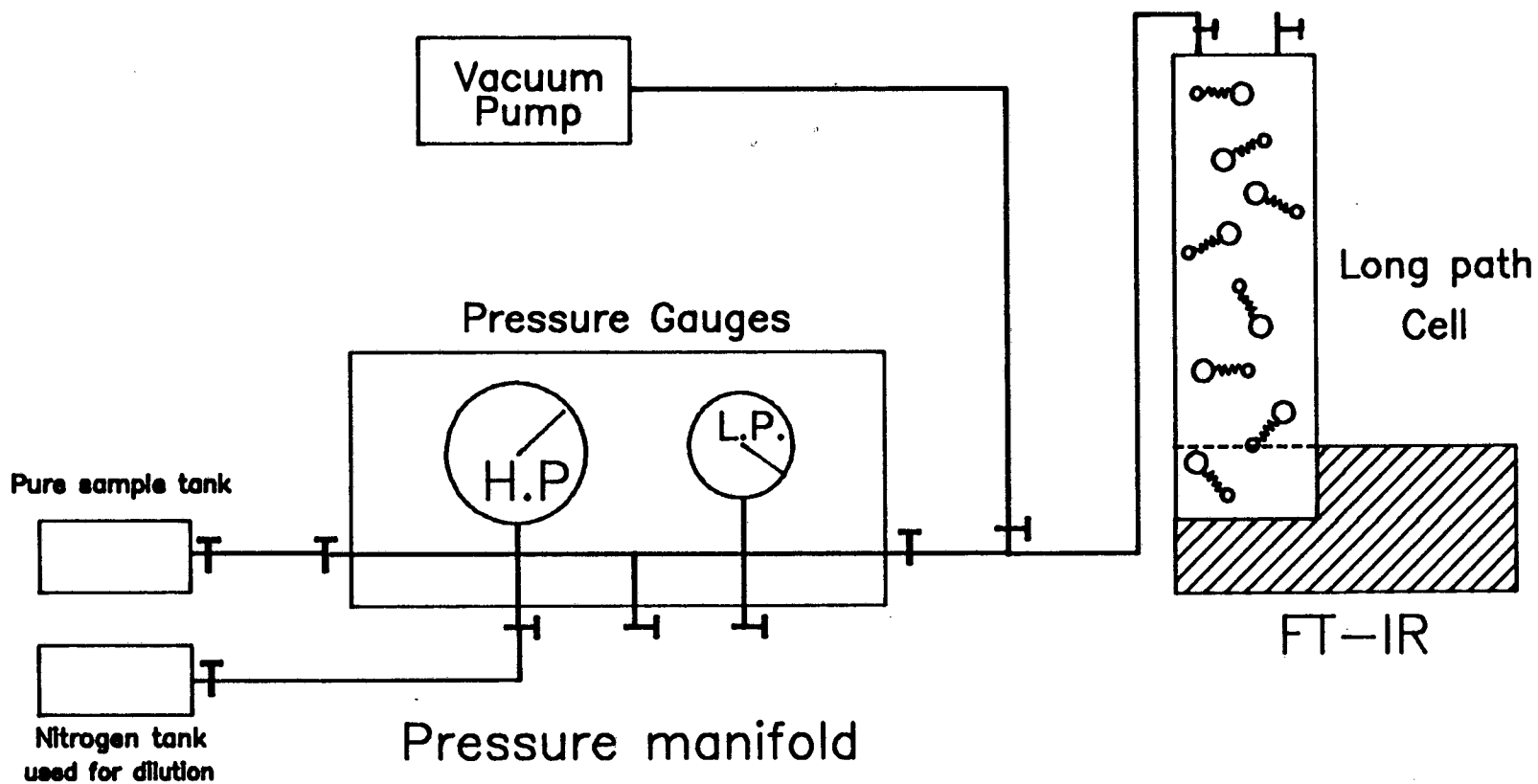
The unexpected behavior of several species, especially those having narrow rotational bands, was a consequence of the instrument resolution.

Measuring single peak heights to do quantitative analysis for the species calibration, was not effective because of the random relative peak height changes.

Fig.31 to **37** present the absorbance of several peaks for each species as a function of the optical density (in torr*cm). The samples were prepared using the syringe method with a total pressure equal to 100 torr. All the spectra were taken using 16 scans, the maximum resolution of $0.25cm^{-1}$, with the set for aperture $0.5cm^{-1}$, and the boxcar apodization function. The optical density was varied, by injecting different concentrations, or by varying the number of passes in the cell. These charts were used as references for our quantitative measurements of the combustion products.

Fig.10

CALIBRATION SYSTEM

Vacuum
Pump

Pressure Gauges

H.P   L.P.

Pure sample tank

Pressure manifold

Nitrogen tank
used for dilution

Long path
Cell

FT—IR

III.3.3. Instrument resolution effect on the
species absorbance:

The operating resolution depended upon two factors: the resolution selected up in the menu which determines the total displacement of the moving mirror in the Michelson interferometer, and the spacial aperture at the spectrometer focal plane.

For all species, we obtained higher absorption and narrower rotational line width by increasing the resolution. **Fig.11** shows the effect of the instrument resolution on the HCl absorbance at 2844 cm^{-1}. The concentration of HCl was equal to .17 torr diluted in 100 torr of nitrogen. Spectra from the same sample were taken with different resolutions. The absorption of the HCl rotational lines were found to be four times lower at 2 cm^{-1} resolution than at 0.25 cm^{-1} resolution. Also, the absorbance was doubled (see **Fig.12**) by operating with a small aperture (0.5 cm^{-1}) in comparison to the open aperture. However, the capability to distinguish between two close rotational lines is not improved. For HCl, we started to see an overlap between the two isotope rotational lines, separated by 2 wavenumbers, at a resolution of 2 cm^{-1} using two different aperture.

III.3.4. Effect of the total pressure on the absorbance:

The effect of the total pressure on the species absorbance was examined by adding nitrogen to the cell. Most of the species were strongly affected by varying the total pressure. Absorbances for water, carbon dioxide, carbon monoxide, hydrogen chloride, ethylene, and acetylene could vary by a factor of three for changes of total pressure between 10 and 760 torr. The absorbance behavior was contrary to theory which predicts that pressure broadening effects, would tend to decrease the peak absorbance. In the pressure range used, ethyl chloride and propane were the only species having smaller absorbances as the total pressure increased, because these species have larger band width.

Shifts in frequency of the peak absorption for some species were observed to exceed 0.5 to 2 wavenumbers, when the total pressure was increased. For example, hydrogen chloride, a shift of 1.2 wavenumbers was observed when the total pressure was increased from 5 to 100 torr.
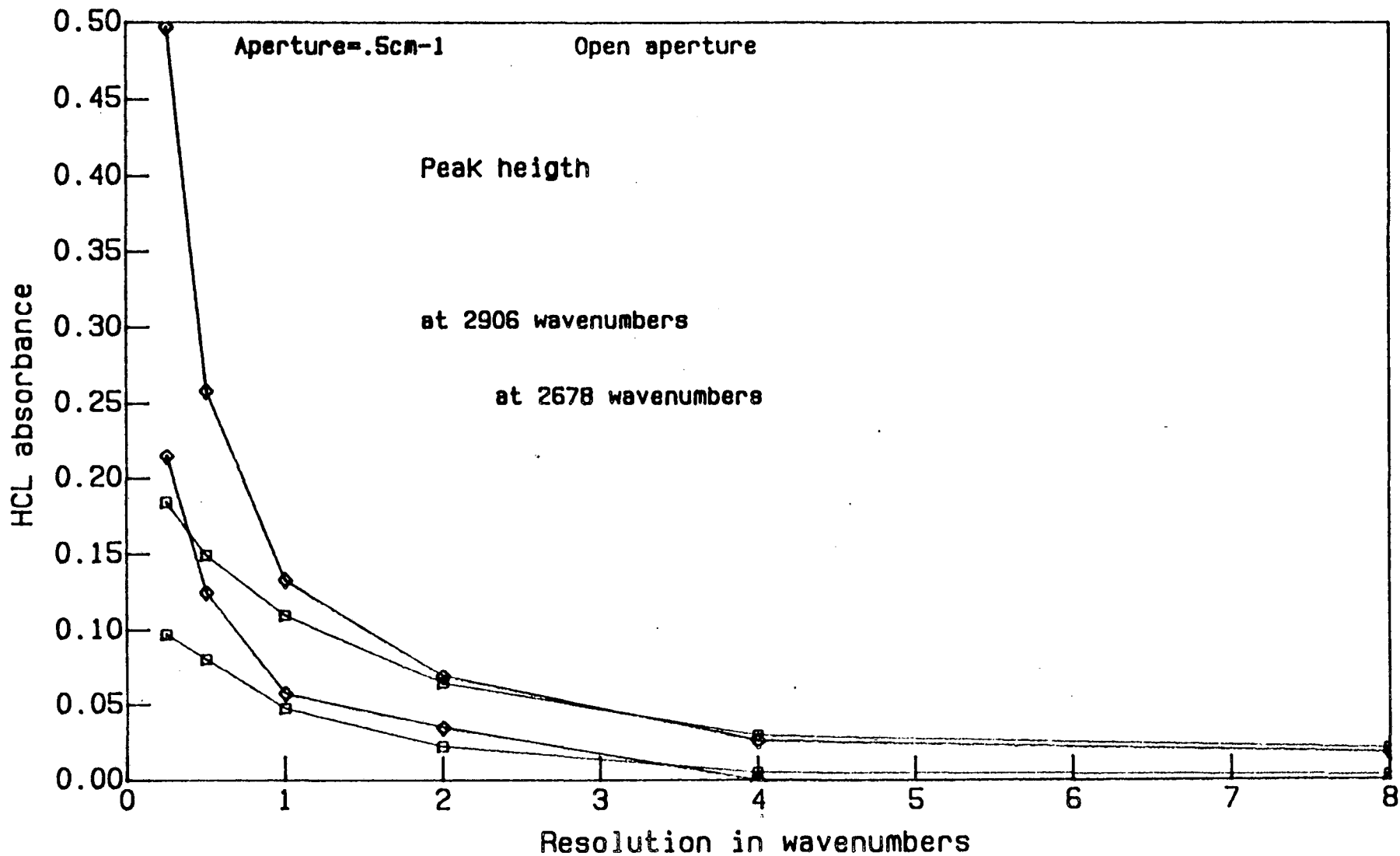
40

Fig.11
UCB

2 wavenumbers res.

Absorbance
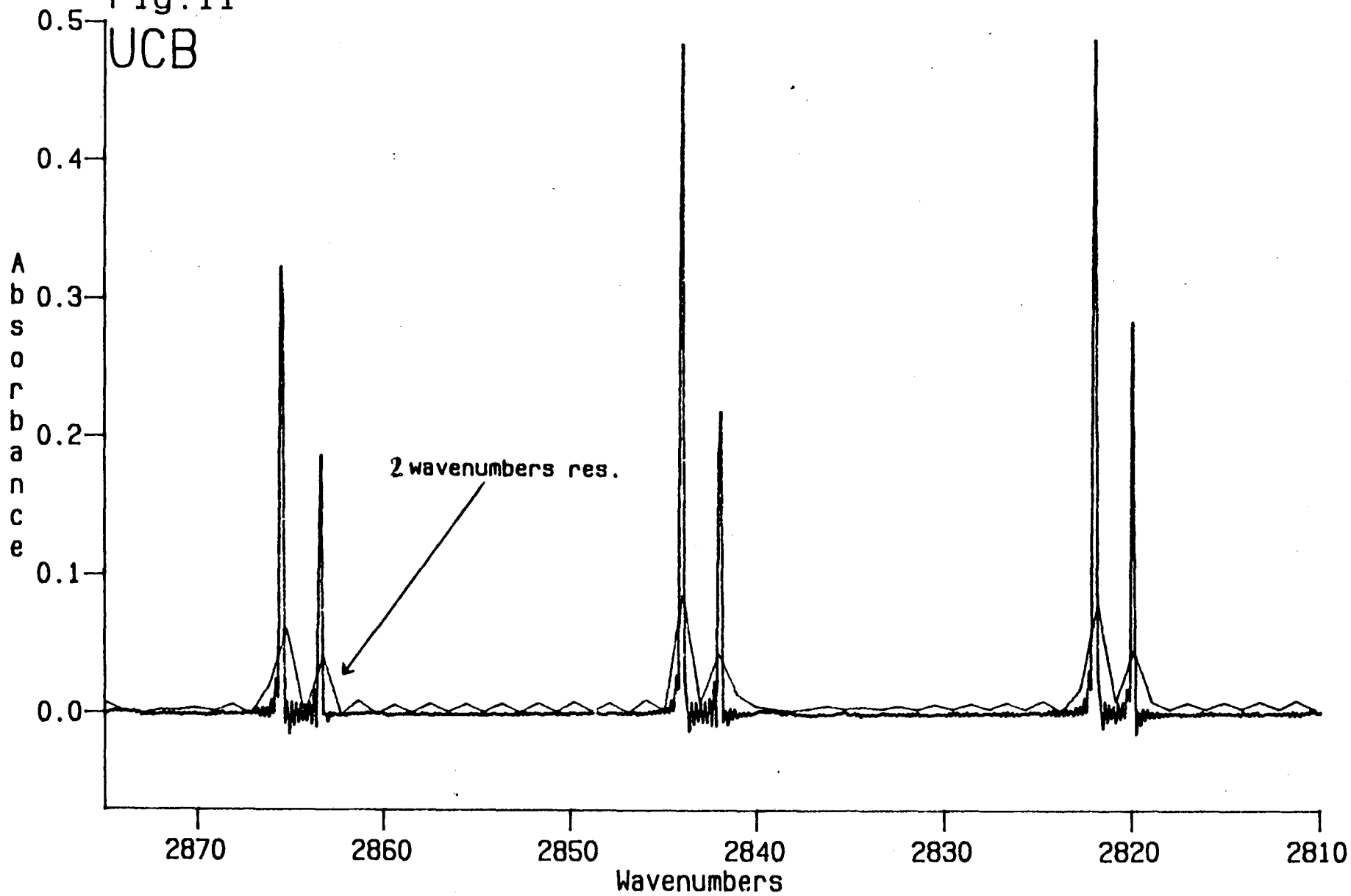
Wavenumbers
HCL
.17 torr of HCL diluted in 100 torr of N2; Aperture=.5 cm-1; 4 Passes
RES=0.25

Fig.12

Effect of the instrument resolution on the hydrogen chloride absorbance
Sample: .17 torr of HCL diluted in 100 torr of Nitrogen

The relative peak height of an absorption band was also affected by variations of the total pressure; the maximum absorption of a rotational band was shifted from one line to another.

Fig.13 to **15** show the behavior of the carbon monoxide with respect to total pressure variations. In each spectrum the CO concentration is the same but the total pressure was changed by adding nitrogen to the cell.
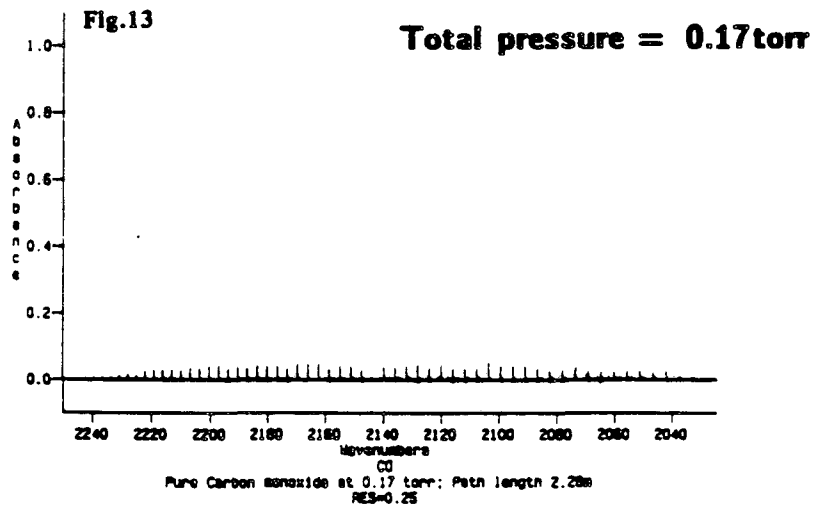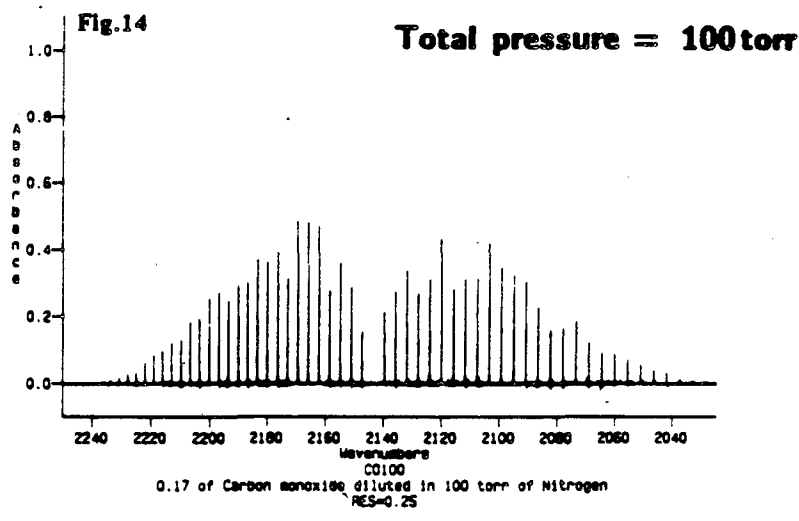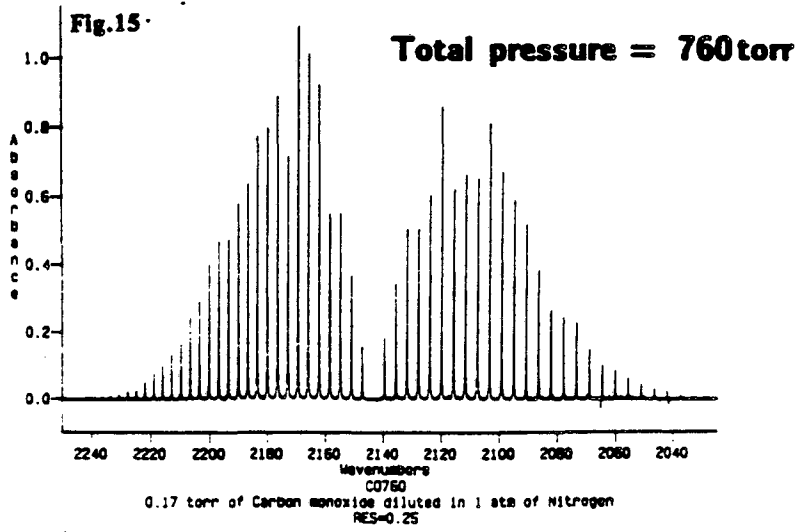
III.3.5. Detectability limits:

Detectability limit tests were performed on hydrogen chloride and ethyl chloride; 100 μl of each sample was injected into the cell diluted with nitrogen until a total pressure of 1 atm was reached. After 30 minutes the cell was evacuated to a low pressure (between 2 and 5 torr depending on the desired concentration of the sample) and then refilled with nitrogen to 100 torr.

Fig.16 and **17** shows a spectrum of 4×10^{-5} torr of hydrogen chloride taken at a resolution of 0.25 cm^{-1} (aperture = 0.5cm^{-1}) at 8192 scans, 48 passes were set in the multi-pass cell.

Scanning lasted more than five hours (it takes about five second per scan at the highest resolution and at 20khz mirror velocity). The signal-to-noise ratio was more than 7. Since hydrogen chloride sticks to the inside walls of the cell, we measured less than 4×10^{-5} torr. Experiments showed that, HCl absorbances from the same sample decreased 10 % each 30 minutes.

III.3.6. Molecular absorption characteristic:

The following table lists absorption cross sections for selected species at specified wavenumbers and also their pressure sensitivity. The absorption cross sections are given for an optical density of 100 cm*torr.

Fig.15·

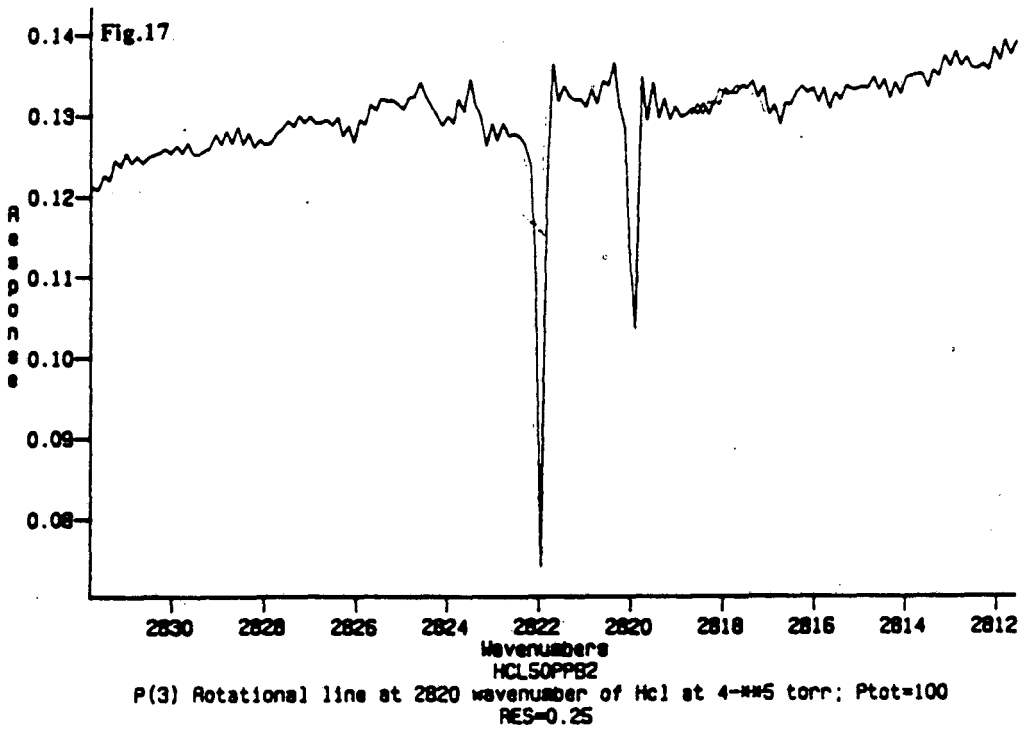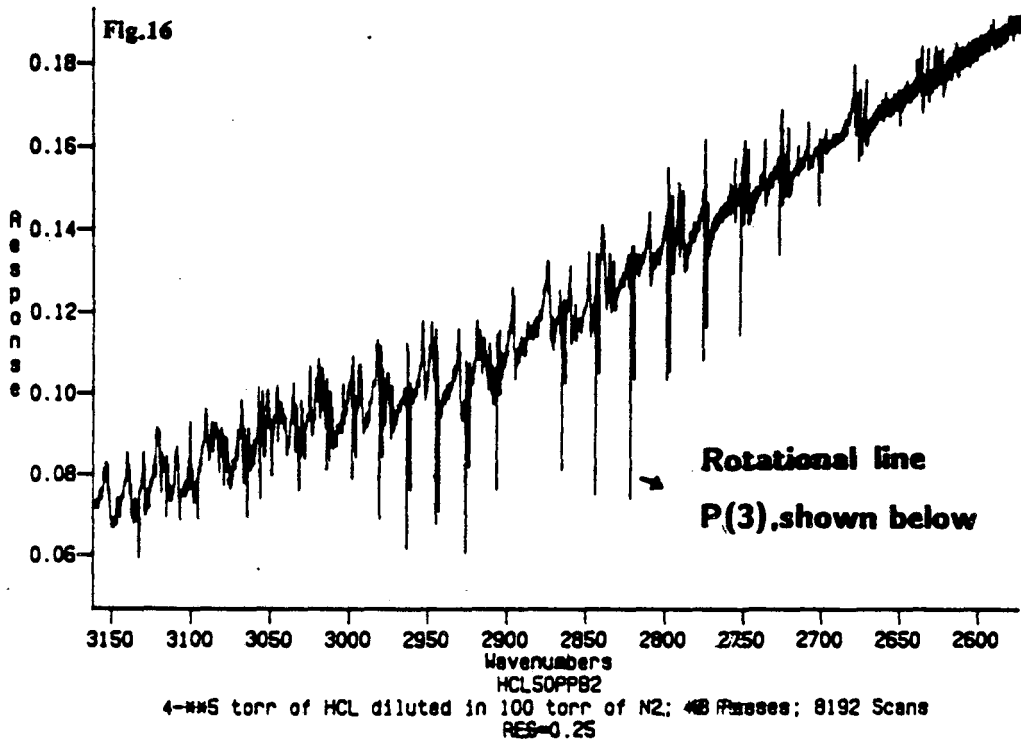**Total pressure = 760 torr**

Wavenumbers
CO760
0.17 torr of Carbon monoxide diluted in 1 atm of Nitrogen
RES=0.25

Fig.14

Total pressure = 100 torr

Wavenumbers
CO100
0.17 of Carbon monoxide diluted in 100 torr of Nitrogen
RES=0.25

Fig.13

Total pressure = 0.17 torr

Wavenumbers
CO
Pure Carbon monoxide at 0.17 torr; Path length 2.2mm
RES=0.25

44

Fig.16

Rotational line
P(3),shown below

Wavenumbers
HCLSOPPB2
4-##5 torr of HCL diluted in 100 torr of N2; 4B Passes; 8192 Scans
RES=0.25

Fig.17

Wavenumbers
HCLSOPPB2
P(3) Rotational line at 2820 wavenumber of Hcl at 4-##5 torr; Ptot=100
RES=0.25

45

TABLE IV.

Classified absorption cross section for selected species

Species	Absorption cross section $(cm*torr)^{-1}$	Wavenumbers in cm^{-1}	Total pressure sensitivity
Propane	1.20	2968	NO
Ethane	0.73	2966	WEAK
HCl	0.72	2944	WEAK
Ethylene	0.70	923	WEAK
Methane	0.67	1306	WEAK
CO	0.55	2166	STRONG
CO2	0.45	647	STRONG
C_2H_5Cl	0.34	1289	NO

III.4. The FT-IR operating conditions used to analyse the combustion products:

In order to identify species and make quantitative measurements from the spectra taken from the sample withdrawn from the tunnel, we have to consider the absorbance behavior of each expected species, which defined the FT-IR operating conditions. Since the species present in the sample had different concentrations and absorption characteristics, we had to take spectra of the same combustion products varying some parameters; e.g. resolution, number of scans, number of passes., etc.

To obtain the maximum resolution from our instrument, we used the smallest aperture ($.5cm^{-1}$) for the IR beam and chose the highest resolution ($.25cm^{-1}$) available.
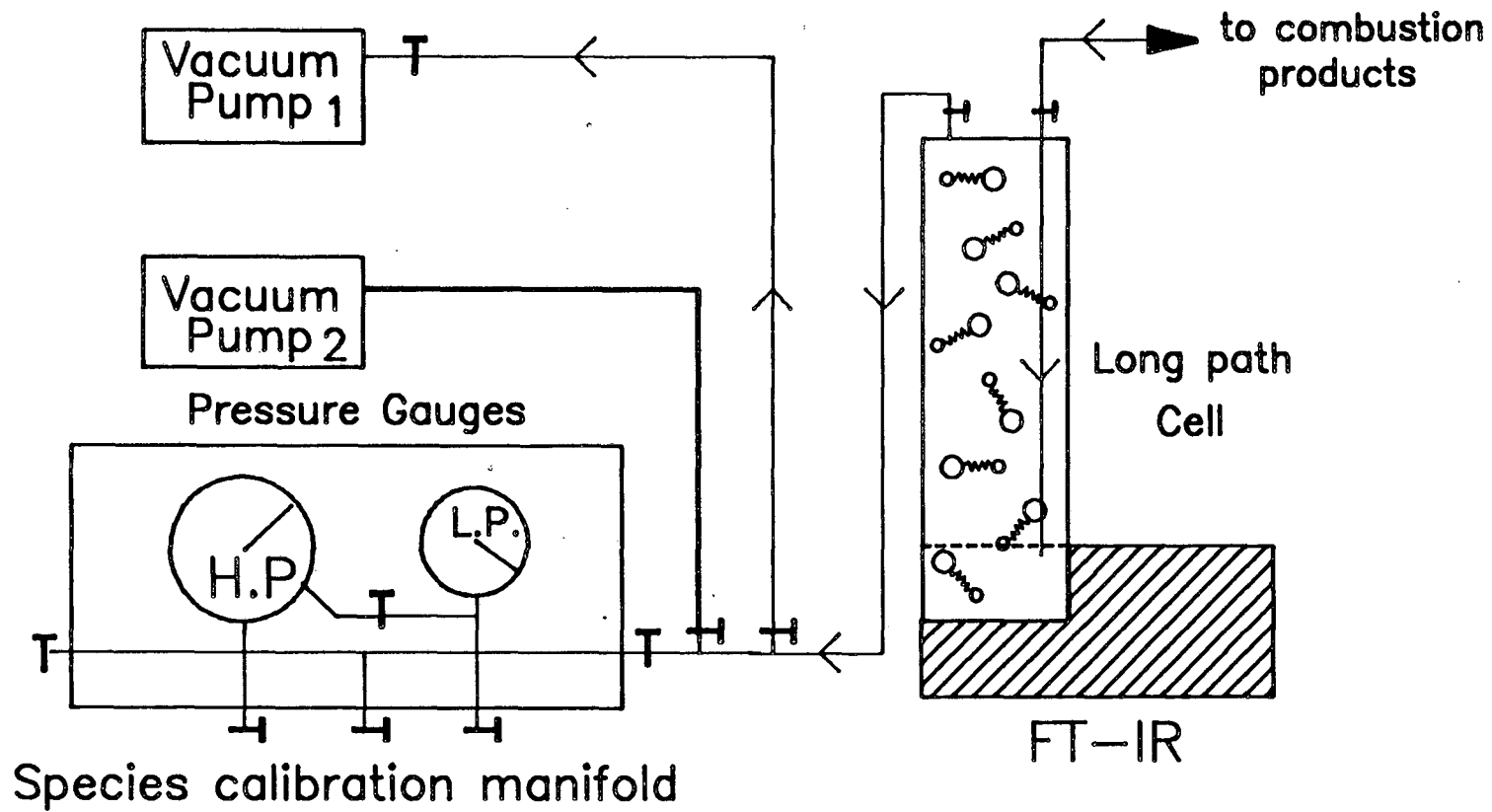
To detect species present in trace amounts, 40 passes (about 23 meters) were used in the long path cell.

All our sample spectra were collected into the cell at a total pressure of 100 torr to prevent water condensation on the walls.

The samples were drawn through the cell at a steady flow rate for 3 to 5 minutes to assure a sample which reflected the composition in the tunnel. See **Fig.18**.

Fig.18

SAMPLE FLOW PATH

Vacuum
Pump 1

Vacuum
Pump 2

Pressure Gauges

H.P

L.P.

Species calibration manifold

to combustion
products

Long path
Cell

FT-IR

IV. RESULTS AND COMMENTS:

Preliminary measurements have been made of species concentrations found in the flow reactor with premixed air-propane, ethyl chloride was injected downstream of the flame (89 cm from the flame holder) at a rate of 0.8 % of the total mass flow rate. Different tunnel operating conditions, included, temperature, equivalence ratio, and Reynolds number.
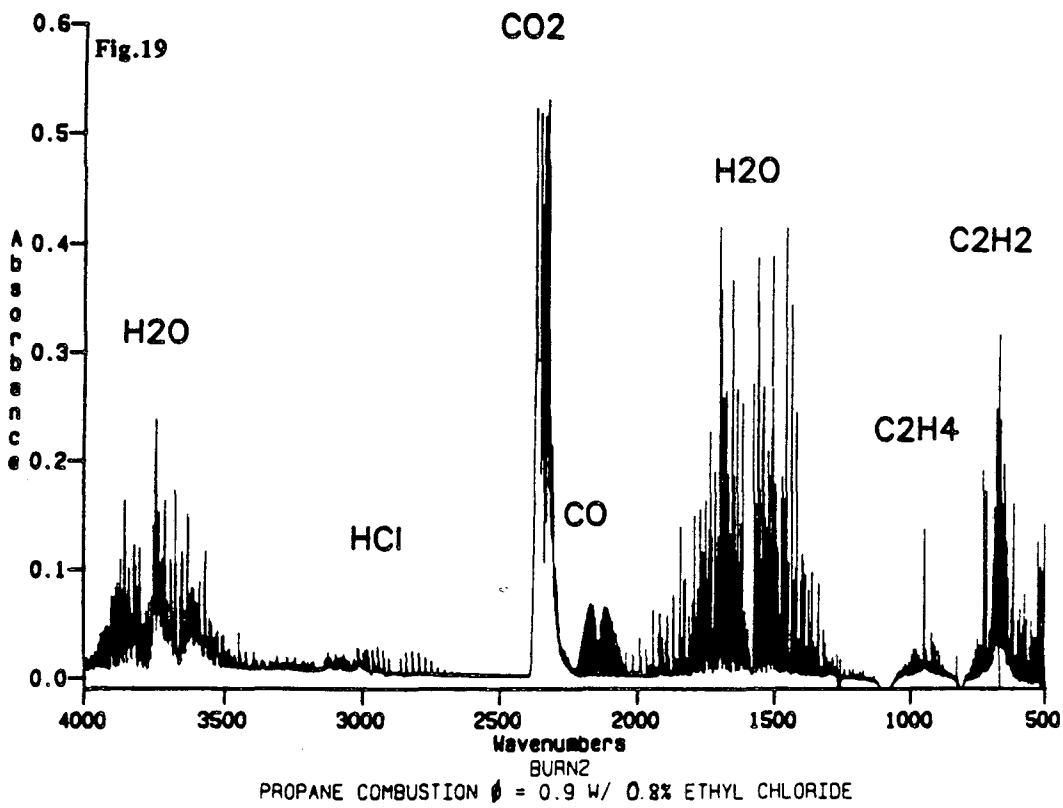
Seven species in the tunnel downstream of the injection point have been identified including: Water, Carbon dioxide, Carbon monoxide, hydrogen chloride, ethylene, acetylene, and ethyl chloride. See **Fig.19**.
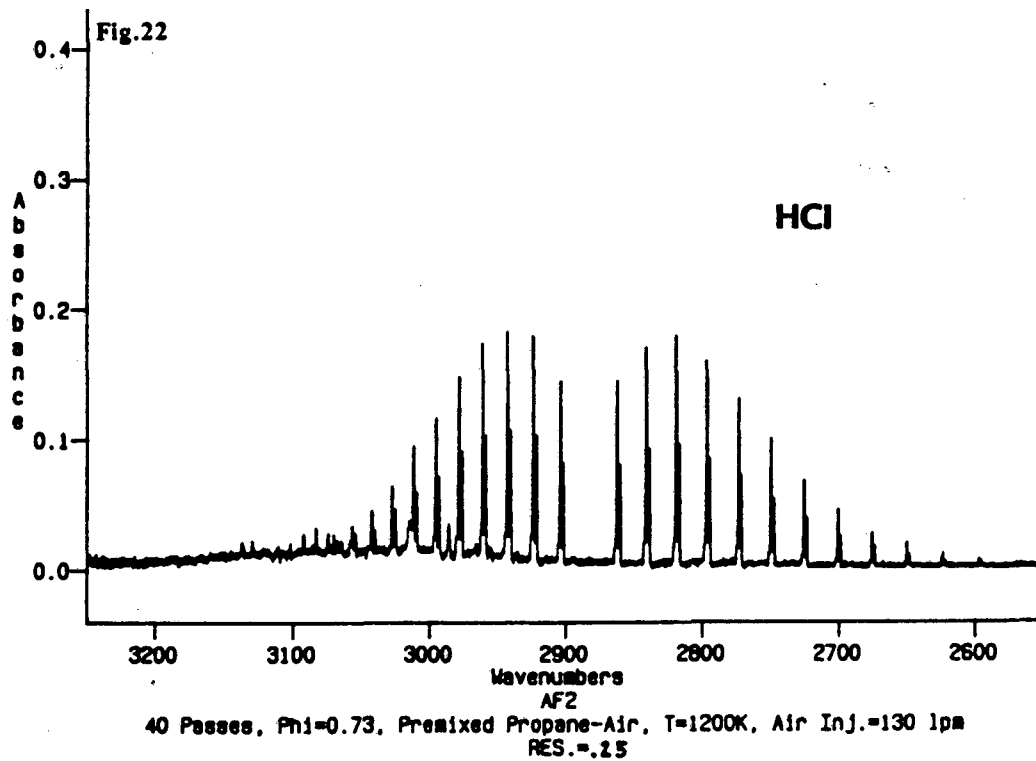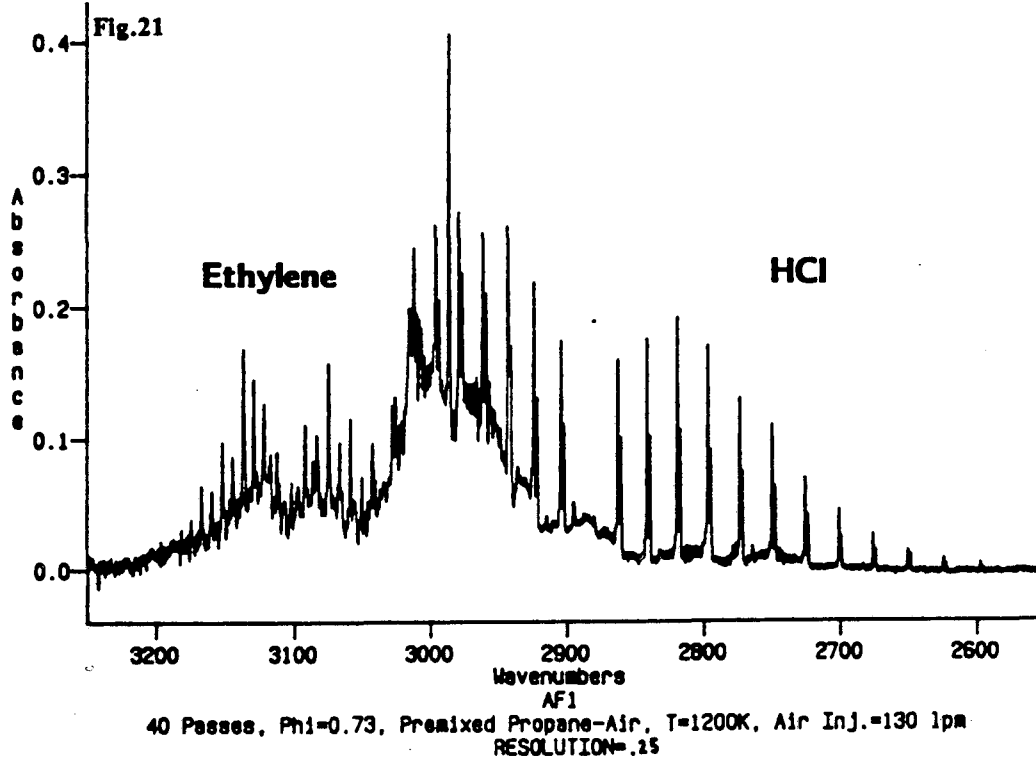
Absorption spectra were calculated using the combustion products without the ethyl chloride injection as the background spectrum. Thus, the spectra reflect only the changes in composition due to the chlorinated hydrocarbon reactions.
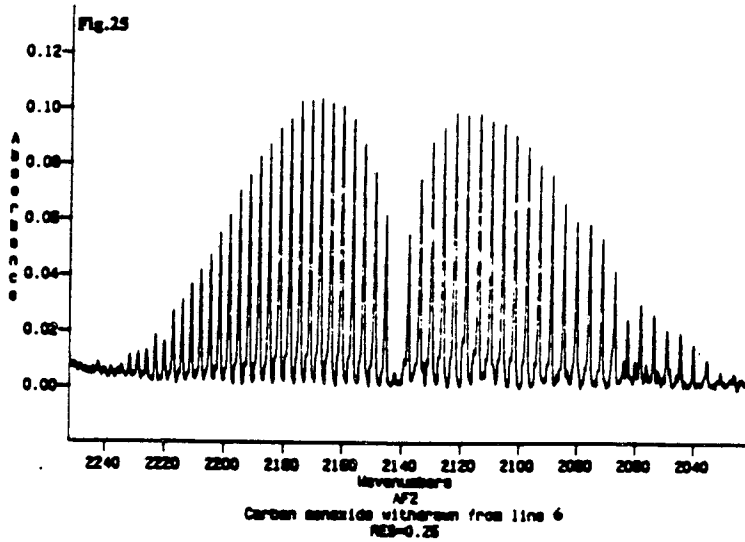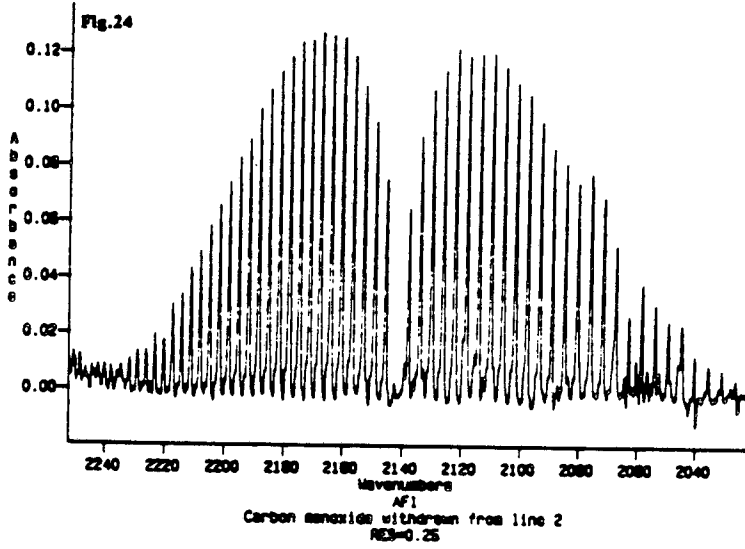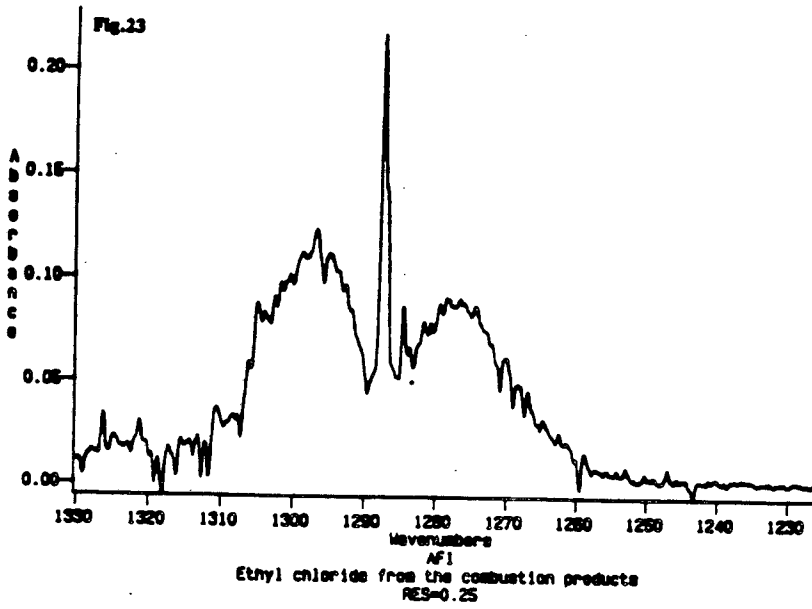
Spectra shown on **Fig.19** and **20** were taken from the combustion product withdrawn from the same sampling line #6 (1.6 meter downstream the ethyl chloride injection). The hydrocarbons and hydrogen chloride detected are the result of the ethyl chloride decomposition. The first presents the species resulting from a lean combustion of propane/air mixture at an equivalence ratio of 0.9, while the second was rich combustion at an equivalence ratio of 1.1. The same amount of ethyl chloride was injected at 1300K ± 40K in both experiments. We noticed increased amounts of ethylene and acetylene due to the partial oxidation of the ethyl chloride in the rich mixture. Concentrations of carbon dioxide and water were also observed to be greater for the rich mixture, while hydrogen chloride concentrations were lower.

Fig.21 to **26** present expanded regions of spectra of combustion products for an air/propane mixture at an equivalence ratio equal to 0.73. The samples were withdrawn from the tunnel at two different locations in order to examine the time history of some species evolution. **Fig.21** shows a spectrum of a sample withdrawn from the flow reactor 10 cm downstream from the point of ethyl chloride injection.
HCl and ethylene were formed rapidly (less than 10 ms); **Fig.22** shows a spectrum withdrawn from the flow reactor 1.6m further downstream. The concentration of HCl remained constant between these two tunnel locations while the ethylene totally decomposed. Ethyl choride was also measured in the sample from the upstream location, **Fig. 23**;

49

Fig.19

PROPANE COMBUSTION φ = 0.9 W/ 0.8% ETHYL CHLORIDE

Fig.20

PROPANE COMBUSTION φ = 1.1 W/ 0.8% ETHYL CHLORIDE

Fig.21

Ethylene

HCl

Wavenumbers
AF1

40 Passes, Phi=0.73, Premixed Propane-Air, T=1200K, Air Inj.=130 lpm
RESOLUTION=.25

Fig.22

HCl

Wavenumbers
AF2

40 Passes, Phi=0.73, Premixed Propane-Air, T=1200K, Air Inj.=130 lpm
RES.=.25

Fig.23

AF1
Ethyl chloride from the combustion products
RES=0.25

Fig.24

AF1
Carbon monoxide withdrawn from line 2
RES=0.25

Fig.25

AF2
Carbon monoxide withdrawn from line 6
RES=0.25

more than 99.99 % was destroyed and not detectable downstream. **Fig.24** and **25** show the evolution of carbon monoxide along the tunnel which continue to be oxidized.

Generally, the ethyl chloride was found to break down quickly into hydrogen chloride and ethylene or acetylene. The destruction efficiency of ethyl chloride was more than 99.99 % in all cases.

IV. FUTURE WORK:

In the future we plan to investigate the following:

- Use liquid fuel spray

- Calibrate and inject other gaseous or liquid chlorinated compounds in the flow reactor.

- Compare experimental and numerical results.

CONCLUSION:

This experimental study of toxic waste incineration was one of the first to use a Fourier transform infrared spectrometer. Making quantitative measurements of species concentration was found to be very difficult.

Measurements were very sensitive to operating condition such as:

- the total pressure in the cell
- the optical component alignment (cell mirrors and beam splitter of the Michelson interferometer)
- the sample cell used
- aperture setting
- the resolution of the instrument
- the properties of molecular species (tendency to stick to wall...)
- the interferences with atmospheric contaminants like water and carbon dioxide.

This study yielded valuable information about ethyl chloride decomposition and the time history of the formation and destruction of intermediate species.

The system provided a simple and rapid means of simulating incineration of toxic waste.

BIBLIOGRAPHY

- John R. Ferraro , Louis J. Basile. **"FOURIER TRANSFORM INFRARED SPECTROSCOPY"**. Applications to chemical systems (Academic Press N.Y.1979)

- A.P.Thorne. **"SPECTROPHYSIC"** Science Paperbacks LONDON 1974.

- Clifford J. Creswell, Olaf Runquist **"SPECIAL ANALYSIS OF ORGANIC COMPOUNDS"**. Burgess Publishing Company, St. Paul, Minnesota.1970.

- E.M. Fisher, C.P. Koshland, and R.F. Sawyer. **"NUMERICAL SIMULATION OF THE THERMAL DESTRUCTION OF SOME CHLORINATED C_1 AND C_2 HYDROCARBONS"**. Paper number WSCI 89-33 presented at the Western States Meeting/The Combustion Institute 1989 Spring Meeting, 20-21 March, 1989. Pullman, Washington.

- C.R. Strang, S.P. Levine, and W.F. Herget. **"A PRELIMINARY EVALUATION OF FOURIER TRANSFORM INFRARED (FTIR) SPECTROMETER AS A QUANTITATIVE AIR MONITOR FOR SEMICONDUCTOR MANUFACTURING PROCESS EMISSIONS"**. Am. Ind. Hyg. Assoc. J. 50(2):70-77 (1989)

- Ying Li-shi and Steven P. Levine. **"FOURIER TRANSFORM INFRARED LEAST-SQUARES METHODS FOR THE QUANTITATIVE ANALYSIS OF MULTICOMPONENT MIXTURES OF AIRBORNE VAPORS OF INDUSTRIAL HYGIENE CONCERN"**. Analytical Chemistry 1989, 61, 677.

- T. Hirschfeld. **"QUANTITATIVE FT-IR: A DETAILED LOOK AT THE PROBLEMS INVOLVED"**. Fourier Transform Infrared Spectroscopy. Vol. 2. Academic Press, Inc. 1979.

- P.L. Hanst. **"POLLUTION: TRACE GAS ANALYSIS"** Fourier Transform Infrared Spectroscopy. Vol. 2. Academic Press, Inc. 1979.

55

Working six month at the University of California,
Berkeley, with a research group is a great experience.
During my training, I had to run experiments, to listen, to
argue, to present, all of which gave me an idea of the
research environment and new ways of looking at things in
life.

CALIBRATION CHARTS

**Fig.26   Calibration of Ethyl chloride mass flow controller
for the tunnel injection**
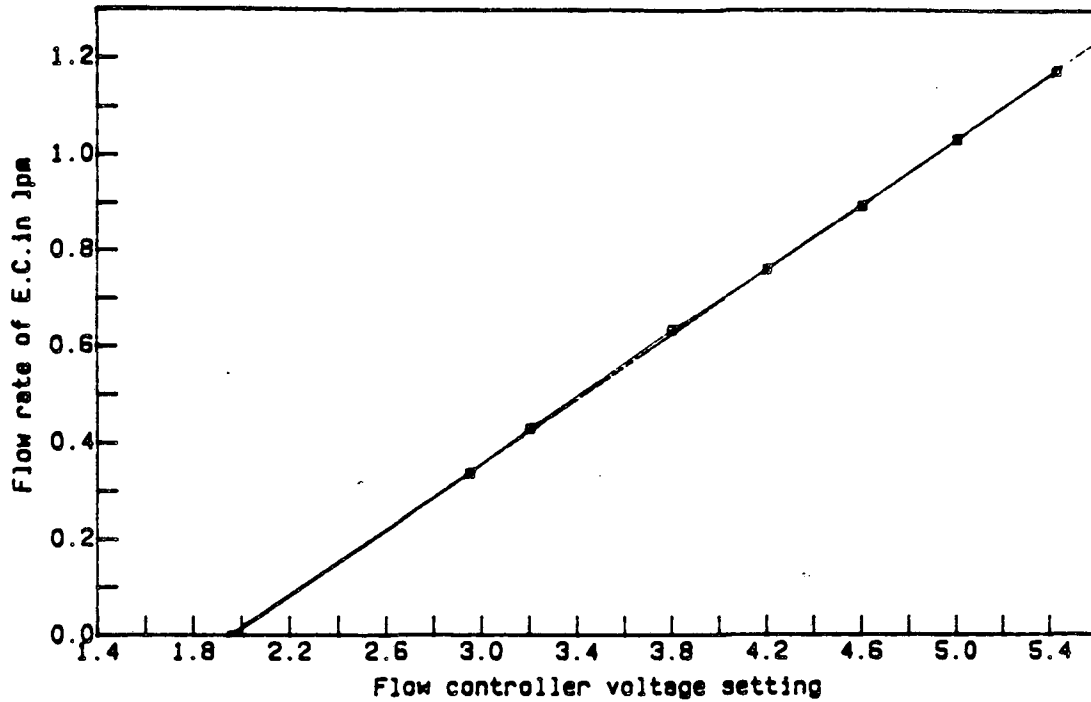
Experimental conditions:

We measured different flow rates for each voltage
set up on the mass flow controller.

Tank pressure: 14 Psi
Line pressure : 9.5 Psi
The water temperature to heat the EC tank was around
100 degrees F

Fitting function based on the experimental data:

$$f(v): = 0.337 \cdot v - 0.6509$$

Where, v is the voltage variable in Volts, and f is the flow
rate in liter/minutes .

Experimental data:

----

f(2.95)= 0.338
f(3.20)= 0.430
f(3.80)= 0.637
f(4.20)= 0.763
f(4.60)= 0.897
f(5.00)= 1.035
f(5.42)= 1.175

Fig.27

Mass flow rate of air versus burrett reading
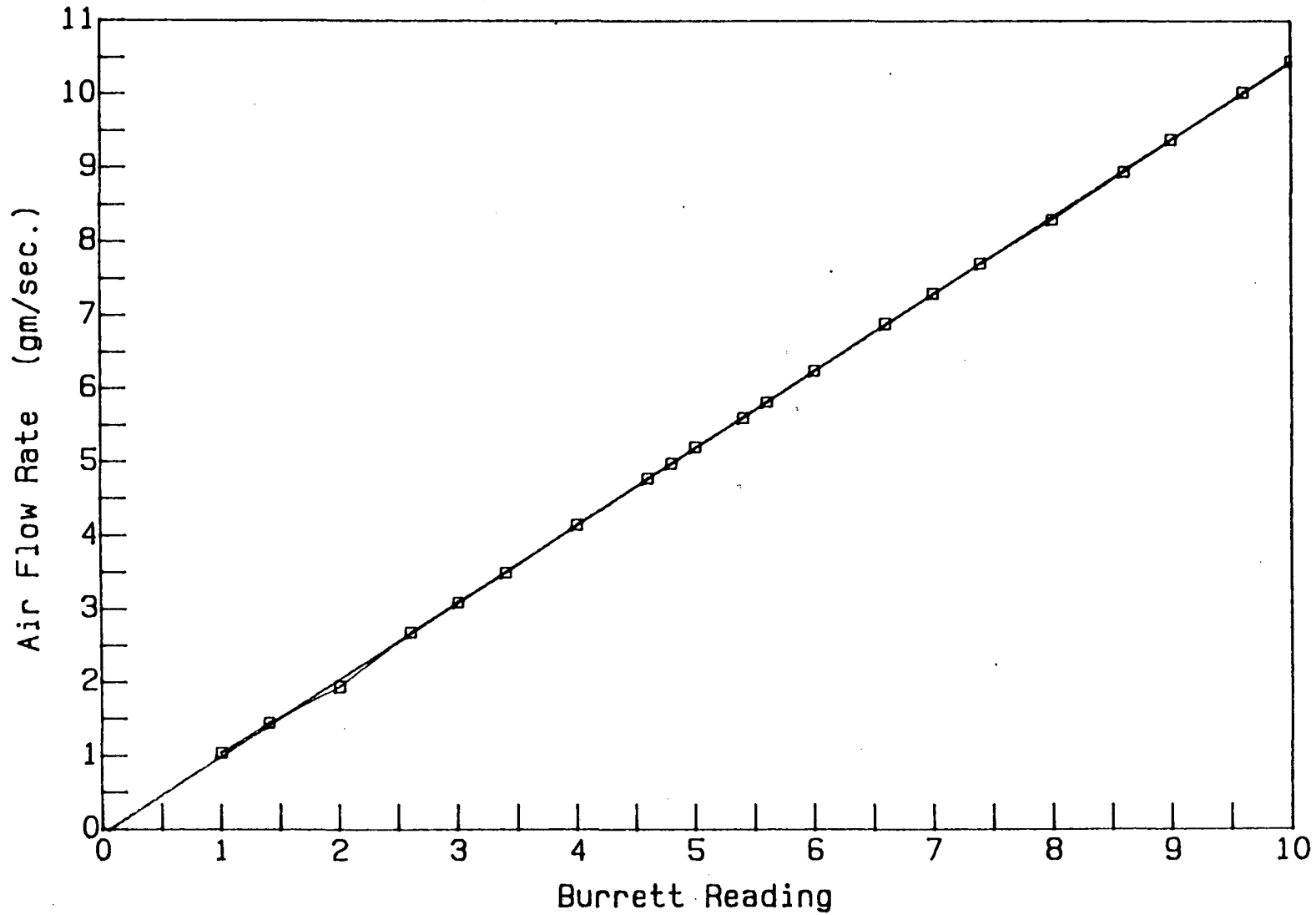
Fig.28

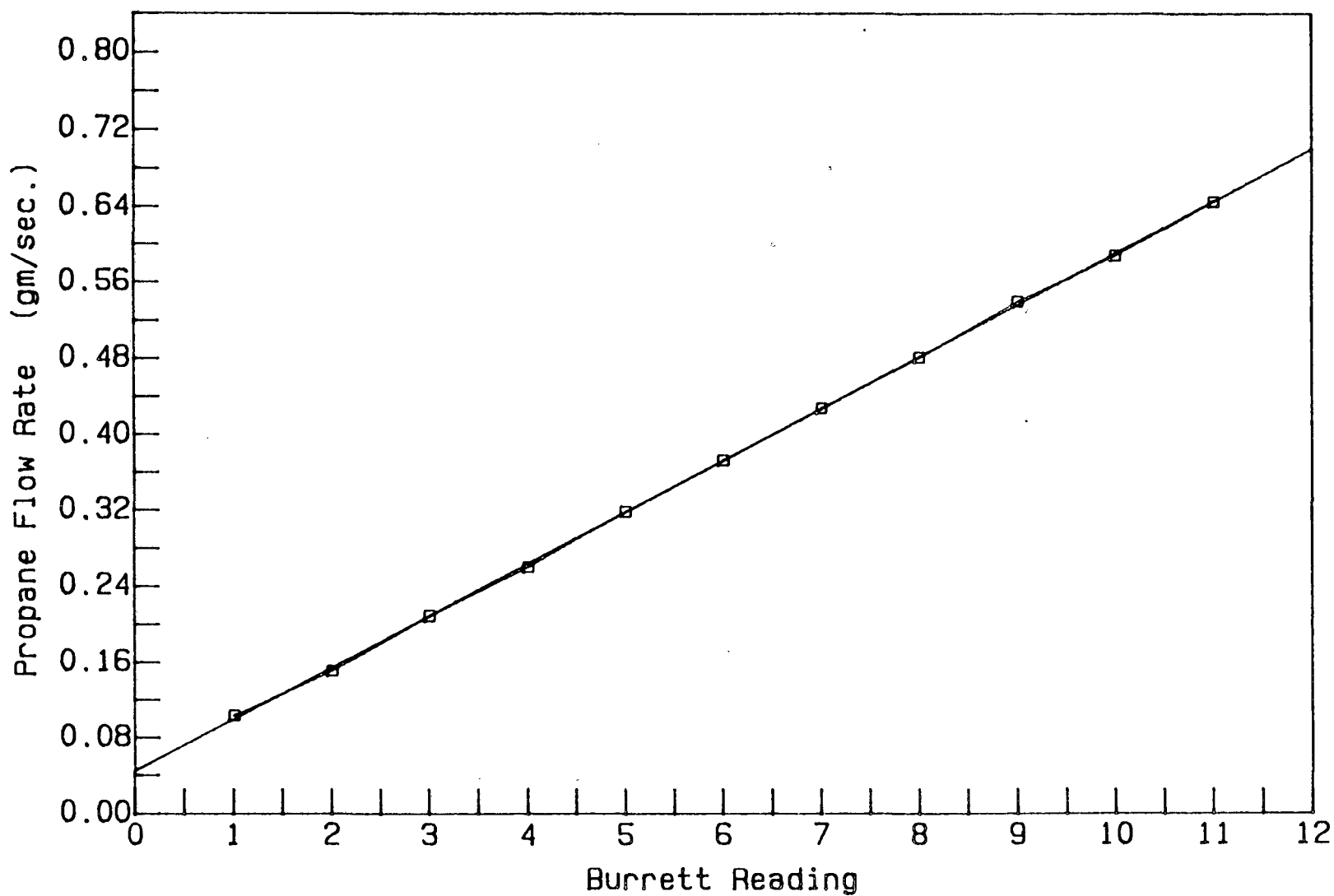Mass flow rate of propane versus burrett reading

Fig.29

Calibration of the manifold pressure gauge

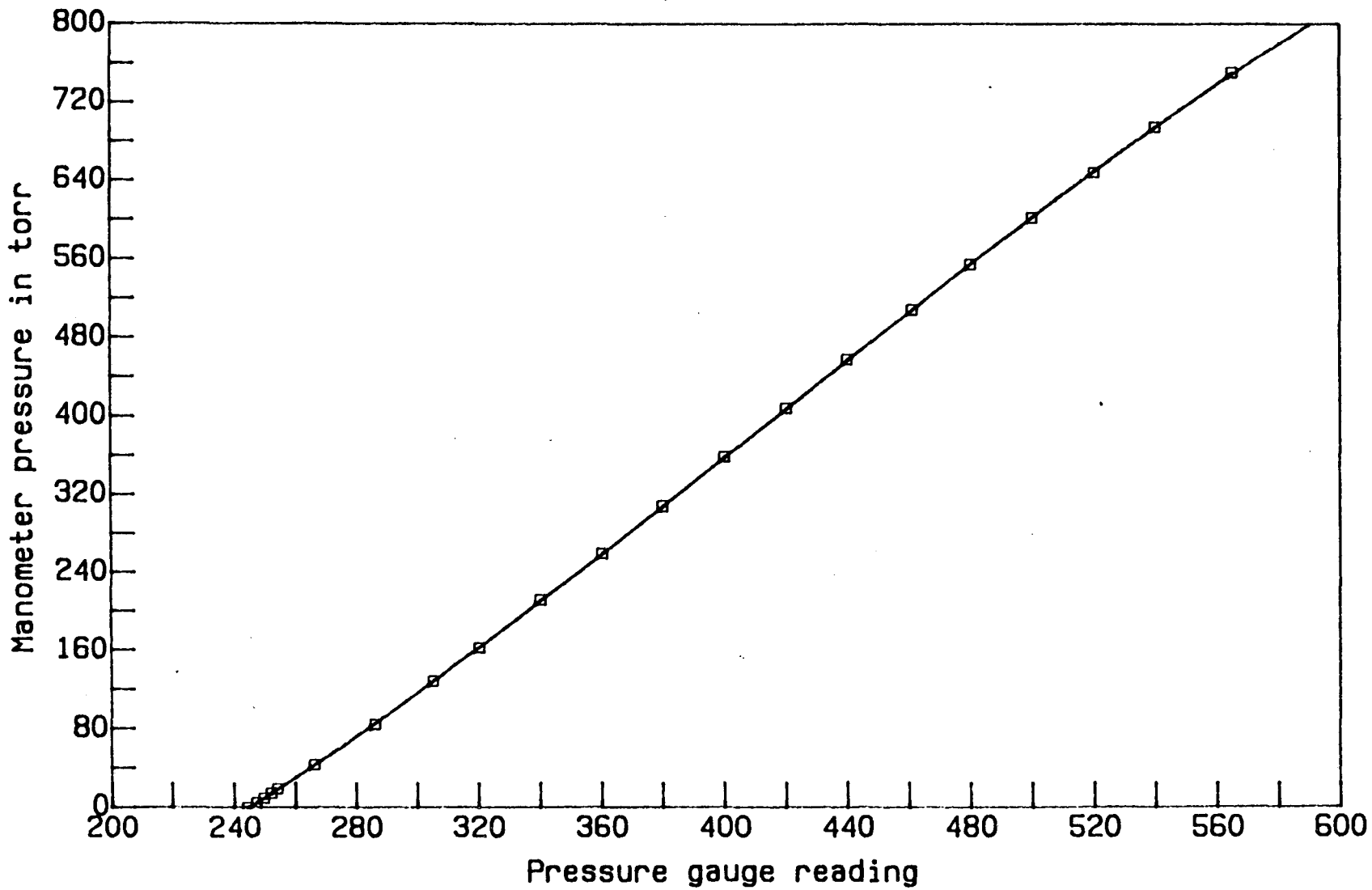used for pressure to 1 atmosphere

Fig.30

Calibration of the manifold pressure gauge

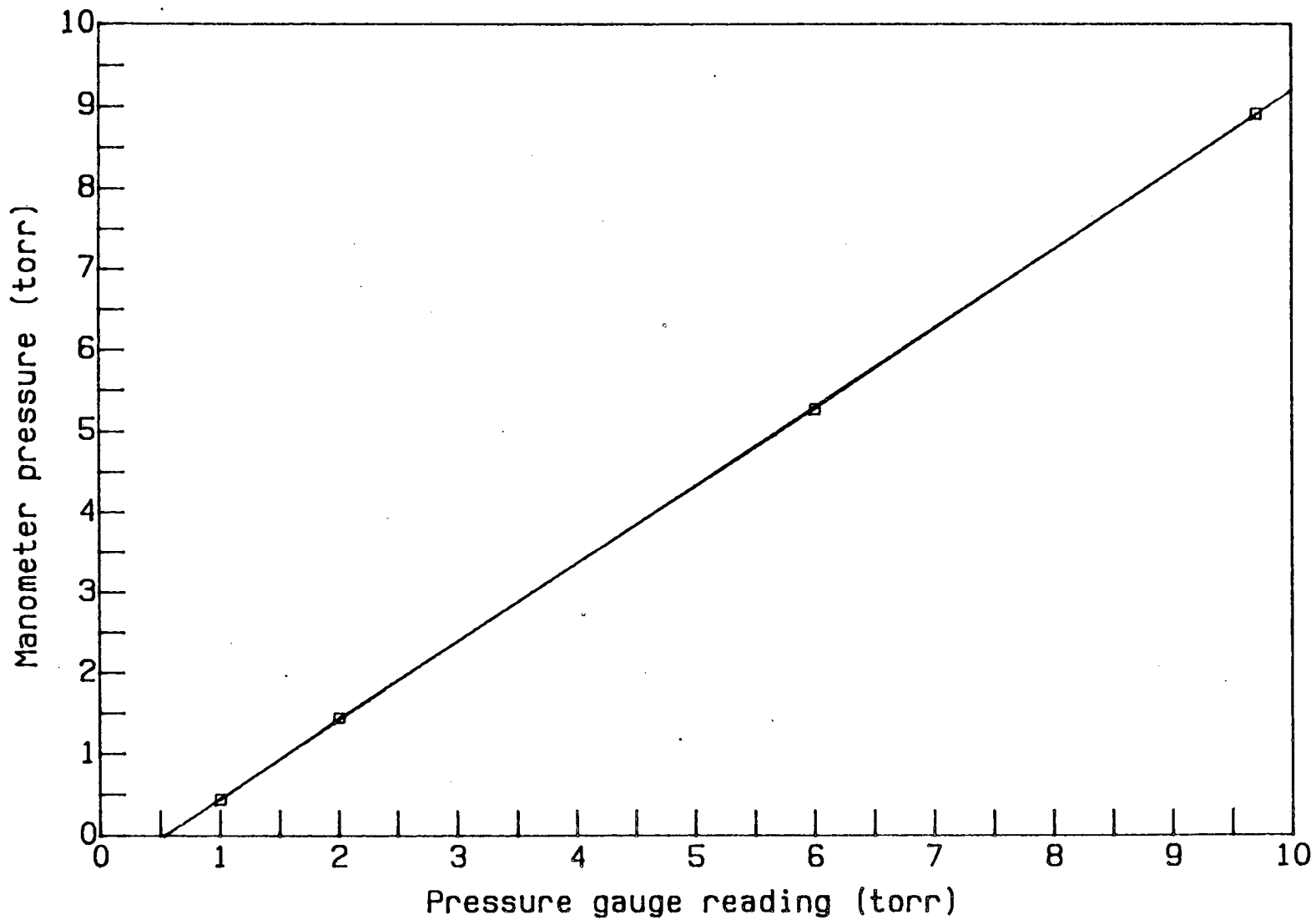for low pressure using a mercury manometer

Fig.31

Effect of the optical density on the carbon dioxide absorbance
at a total pressure of 100 torr balanced w/ Nitrogen
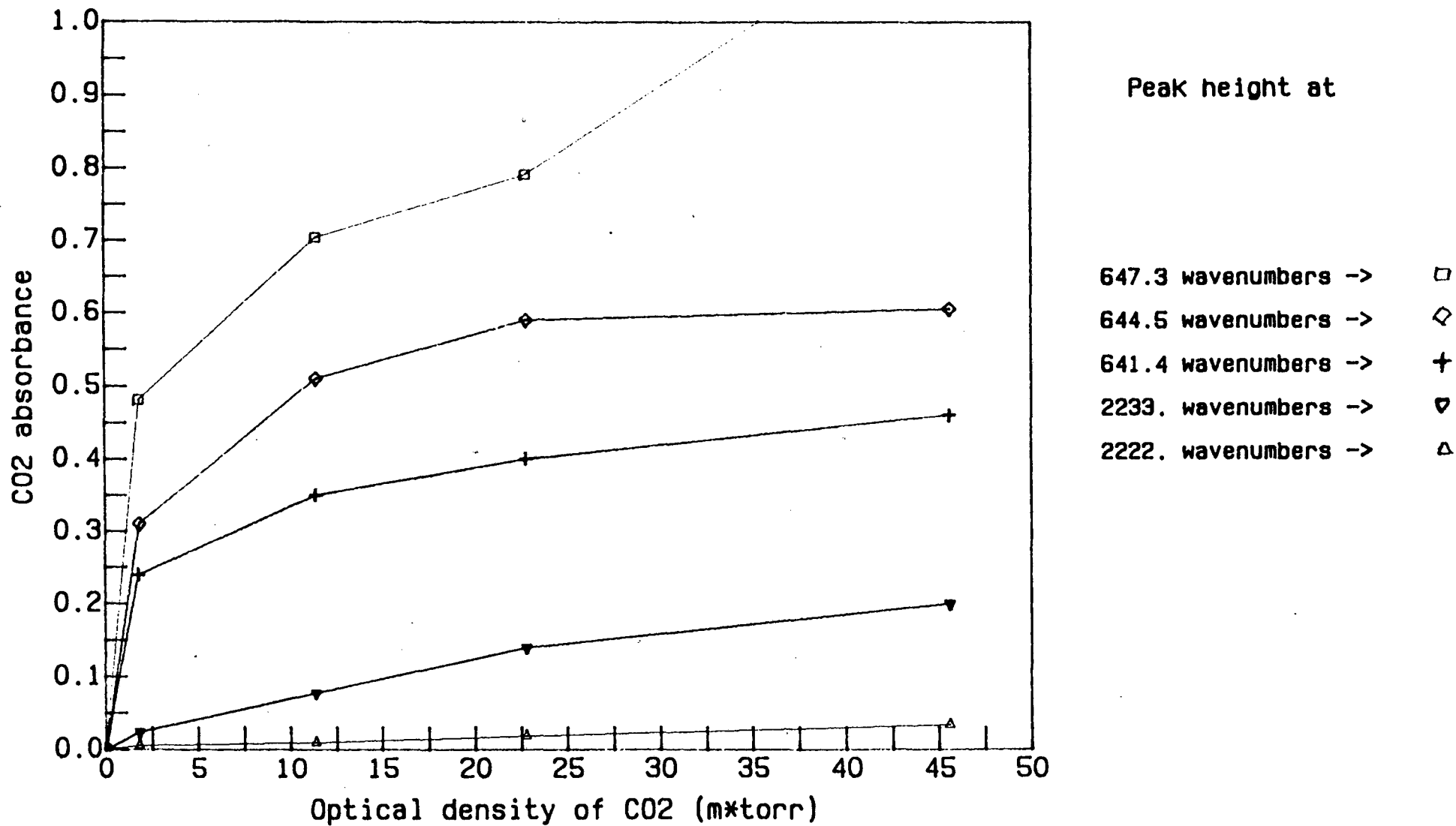Resolution = 0.25cm-1 & Aperture = 0.5cm-1; W/ Syringe injection

Peak height at

647.3 wavenumbers -> □

644.5 wavenumbers -> ◇

641.4 wavenumbers -> +

2233. wavenumbers -> ▽

2222. wavenumbers -> △

Fig.32

Effect of the optical density on the CO absorbance at Ptot 100 torr N2 balanced

Resolution = 0.25cm-1 & Aper.=.5cm-1 ; 16 Scans; Syringe injection

Peak height at

2166 wavenumbers -> □

2073 wavenumbers -> ✕

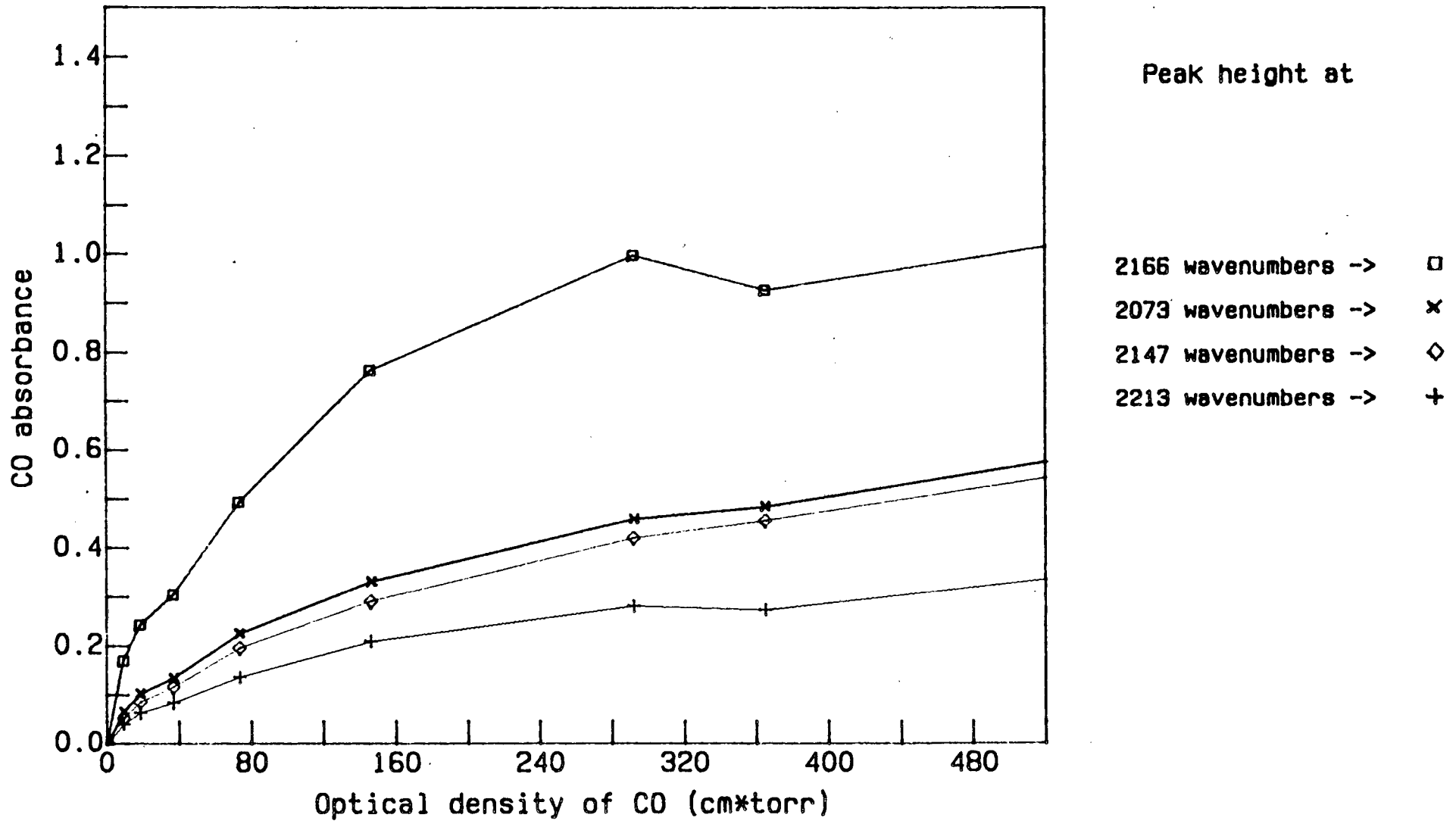2147 wavenumbers -> ◇

2213 wavenumbers -> +

Fig.33

Effect of the optical density on the hydrogen chloride absorbance
at a total pressure of 100 torr balanced w/ Nitrogen
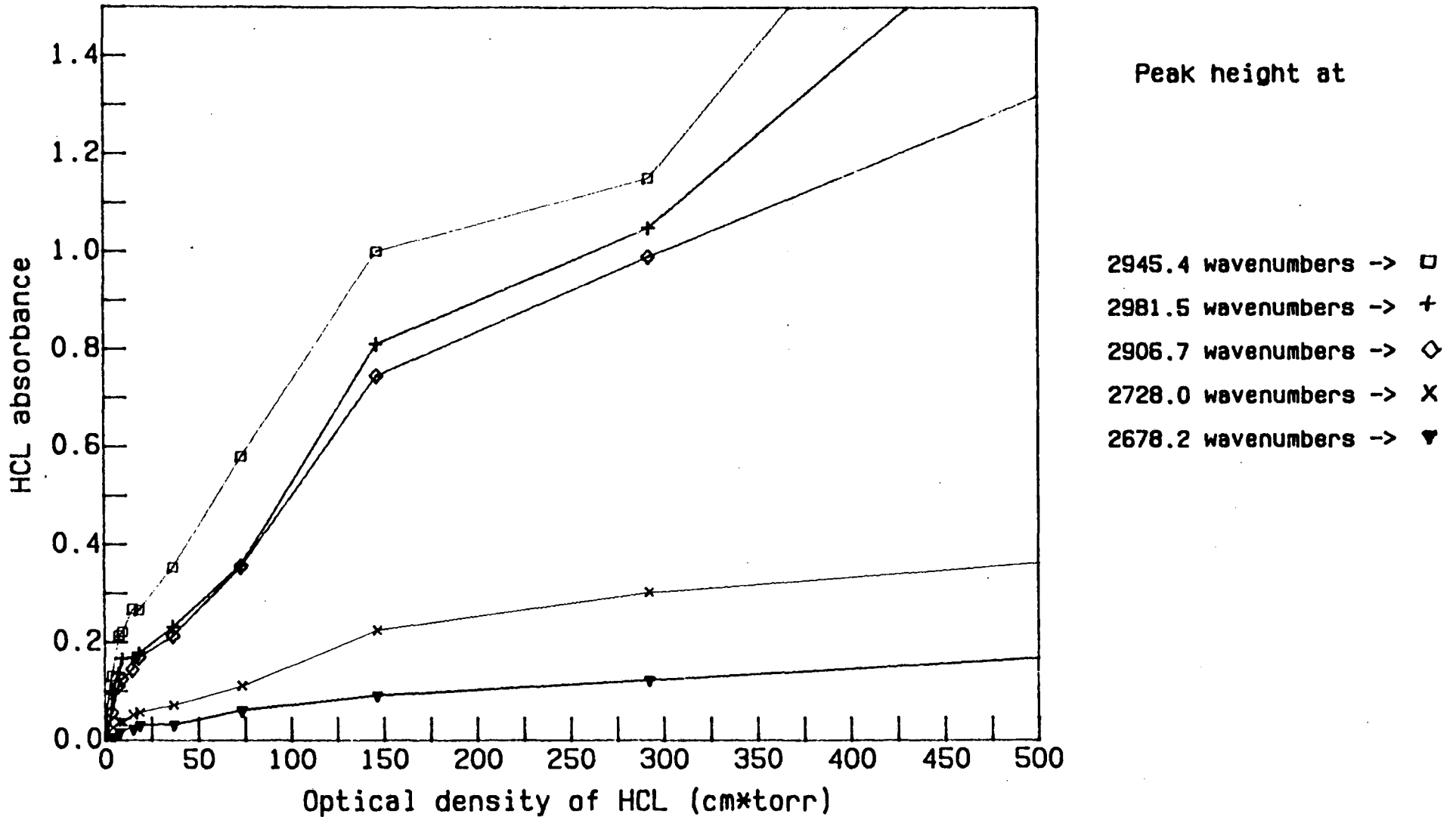Resolution = 0.25cm-1 & Aperture = 0.5cm-1; W/ Syringe injection

Peak height at

2945.4 wavenumbers -> □

2981.5 wavenumbers -> +

2906.7 wavenumbers -> ◇

2728.0 wavenumbers -> ✗

2678.2 wavenumbers -> ▼

Fig.34

Effect of the optical density on the ethyl chloride absorbance
at a total pressure of 100 torr balanced w/ Nitrogen
Resolution = 0.25cm-1 & Aperture = 0.5cm-1; W/ Syringe injection
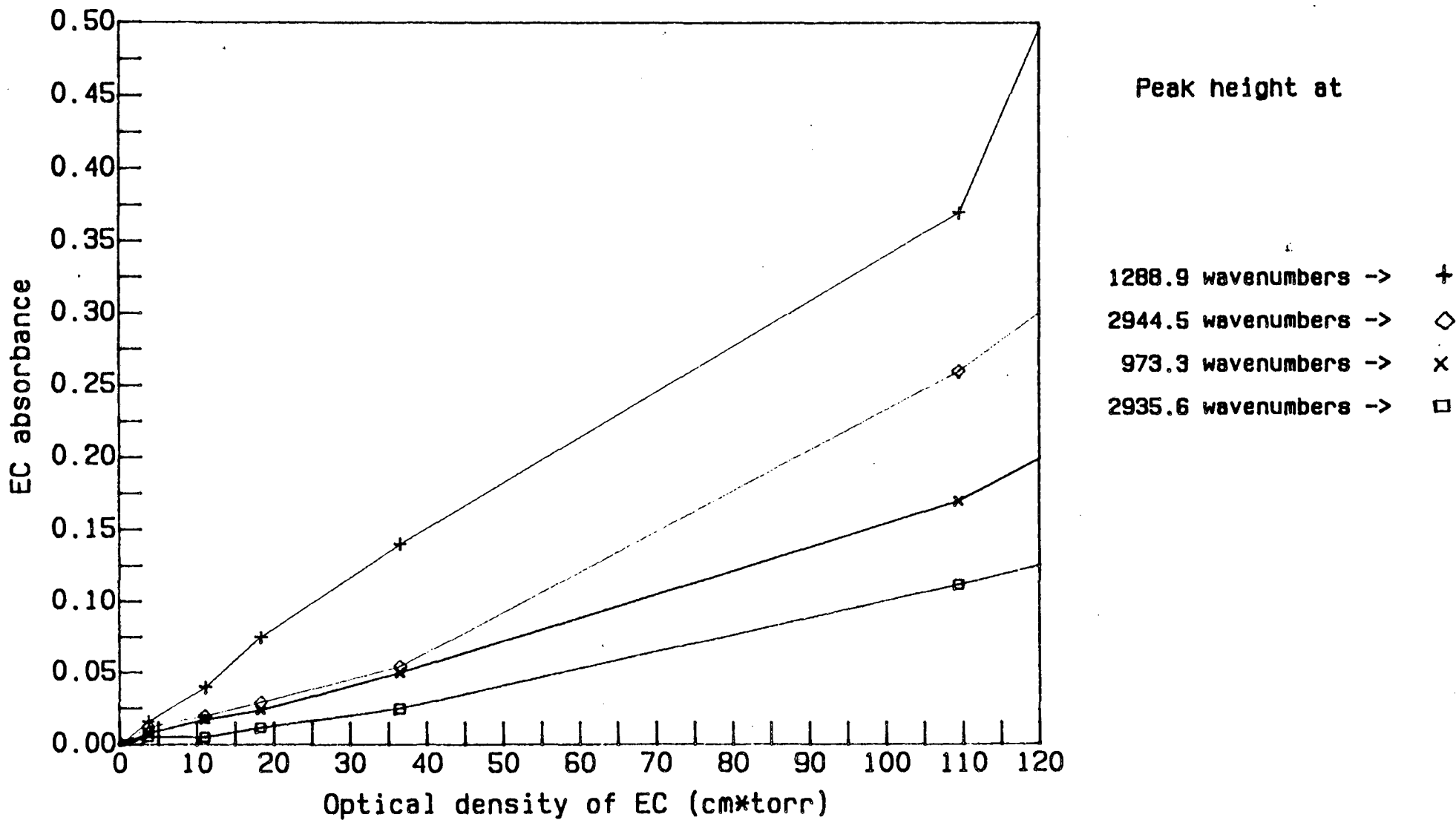

Peak height at

1288.9 wavenumbers -> +
2944.5 wavenumbers -> ◇
 973.3 wavenumbers -> ✕
2935.6 wavenumbers -> ☐

Fig.35

Effect of the O.D. on the Ethylene absorbance at Ptot 100 torr N2 balanced

Resolution = 0.25cm-1 & Aper.=.5cm-1 ; 16 Scans

Peak height at

949.6 wavenumbers ->   ◇
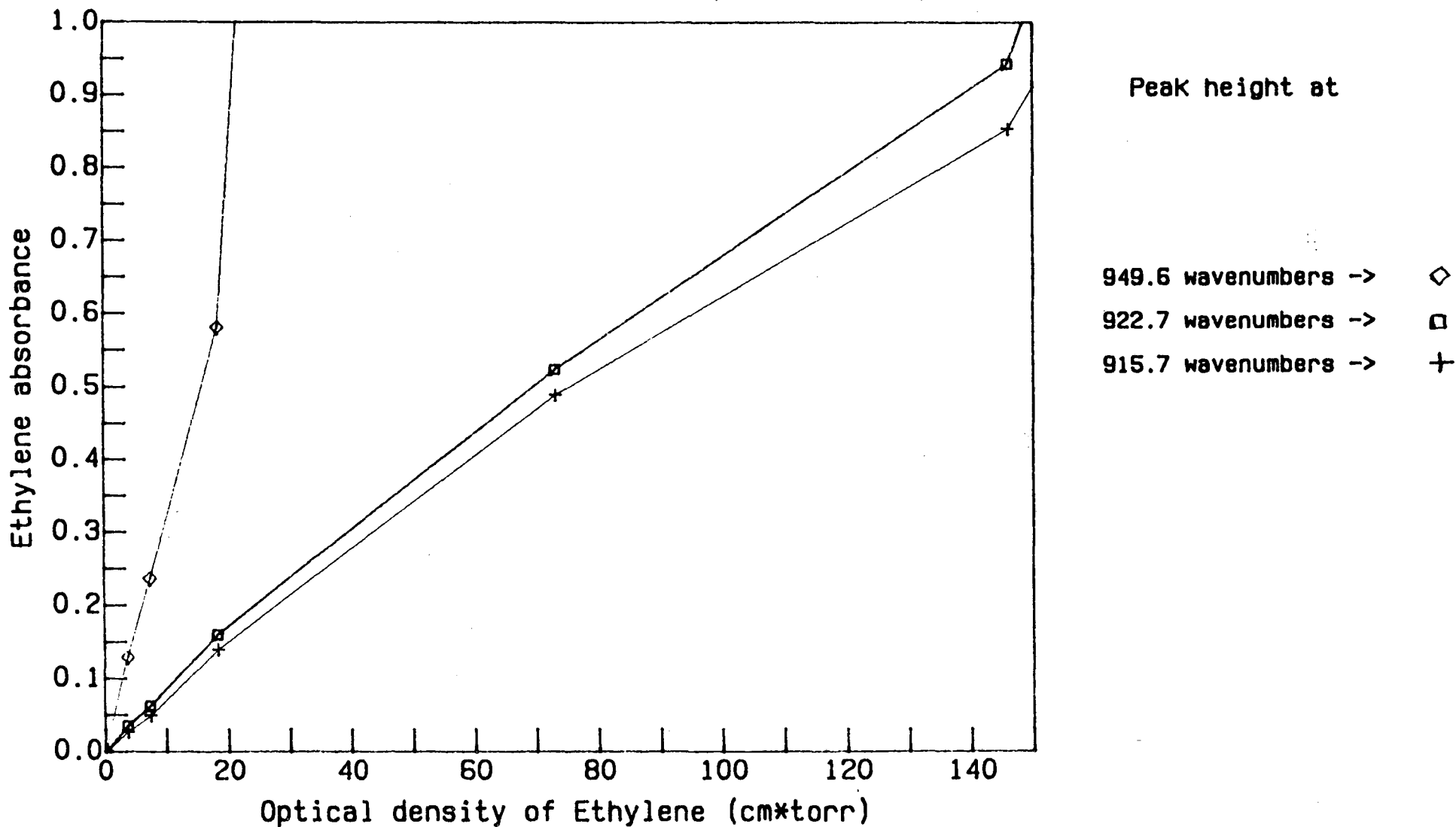
922.7 wavenumbers ->   ◻

915.7 wavenumbers ->   +

Fig.36

Effect of the optical density on methane absorbance at Ptot 100 torr N2 balance

Res=.25cm-1; Aper.=.5cm-1; 16 Scans ; Syringe injection
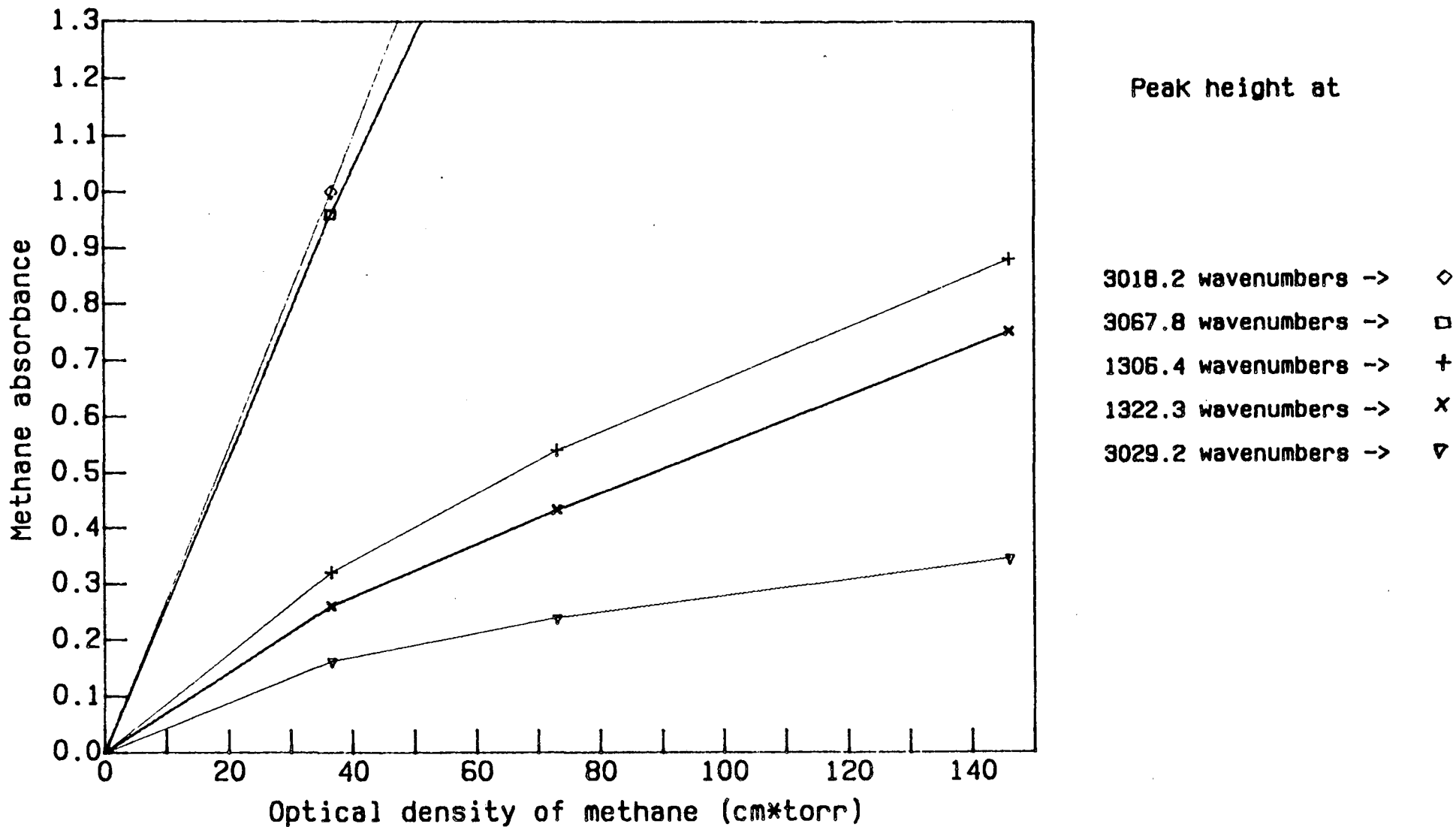

Peak height at

3018.2 wavenumbers -> ◇

3067.8 wavenumbers -> □

1306.4 wavenumbers -> +
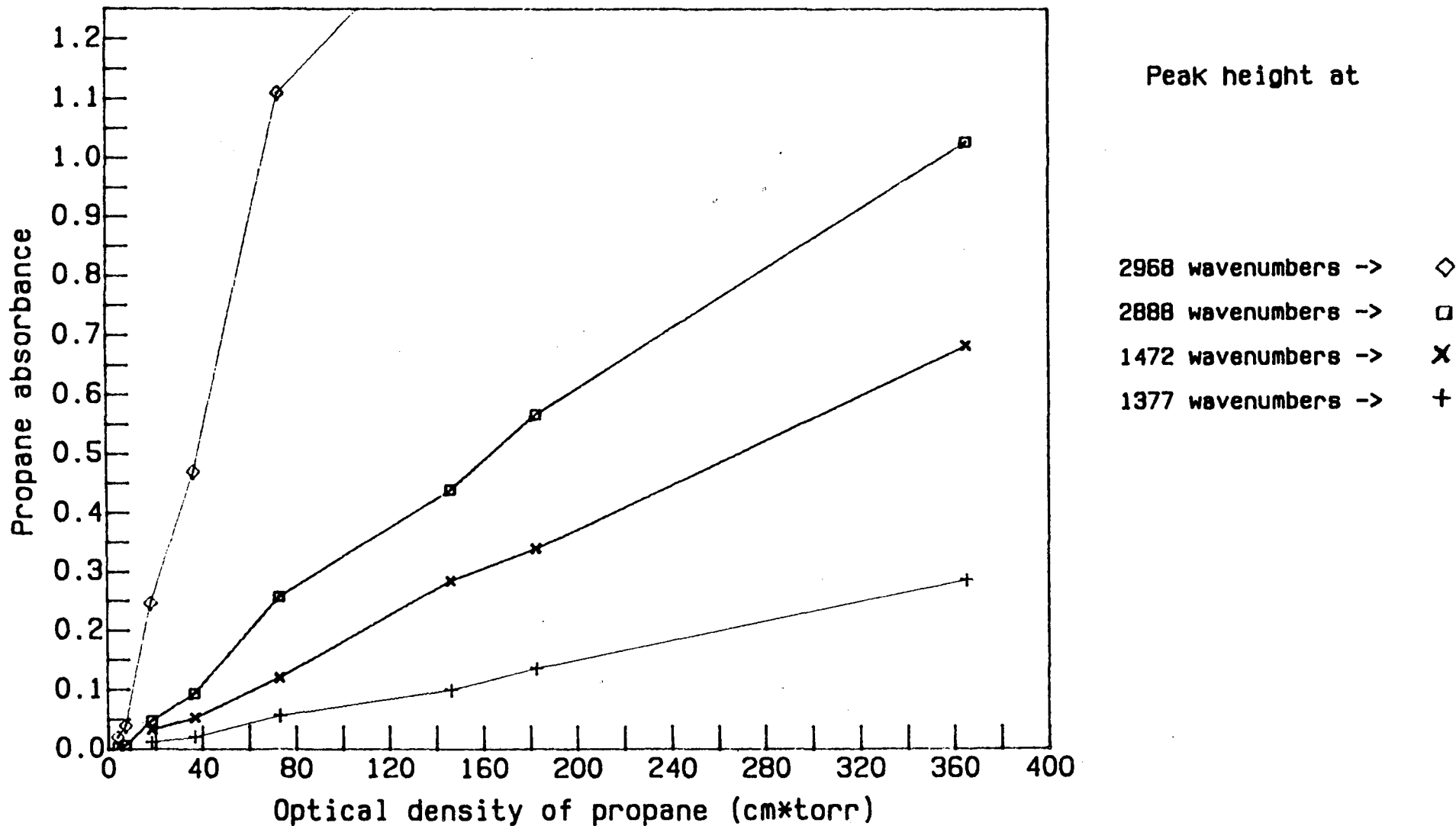
1322.3 wavenumbers -> ✕

3029.2 wavenumbers -> ▽

Fig.37

Effect of the optical density on propane absorbance at Ptot 100 torr N2 balance

Res=.25cm-1; Aper.=.5cm-1; 16 Scans ; Syringe injection

Peak height at

2968 wavenumbers -> ◇
2888 wavenumbers -> ▢
1472 wavenumbers -> ✗
1377 wavenumbers -> +